1.E.1:2.G *Nuclear Physics* A231 (1974) 266—300; © *North-Holland Publishing Co., Amsterdam*

EXCITATION OF TWO-PARTICLE–ONE-HOLE STATES BY THE ^{208}Pb(d, p)^{209}Pb REACTION †

D. G. KOVAR††, NELSON STEIN††† and C. K. BOCKELMAN
Wright Nuclear Structure Laboratory,
Yale University, New Haven, Connecticut 06520

Received 19 November 1973
(Revised 6 June 1974)

Abstract: The weak transitions in the ^{208}Pb(d, p)^{209}Pb reaction leading to two-particle–one-hole (2p-1h) states in ^{209}Pb have been studied at a bombarding energy of 20 MeV. These transfers exhibit typical stripping-type angular distributions and were analyzed using standard DWBA for l-values and spectroscopic factors. Arguments are presented which support an interpretation of these results as one-step transfer reactions proceeding in some cases via single-particle admixtures in the final states and in other cases via 2p-2h correlations in the ^{208}Pb ground state. The results imply a departure of ^{208}Pb from shell closure in qualitative agreement with the magnitude and character predicted by RPA calculations. Four fragments which exhaust most of the available $j_{\frac{1}{2}}$ single-particle strength are observed. Evidence is also obtained for fragments of single-particle strength from the $N > 184$ shell mixed into low-lying states of primary 2p-1h configuration. The observed levels are compared with the ^{209}Pb level structure predicted by calculations based on a hole coupled to the multipole pairing states in ^{210}Pb and a particle coupled to particle-hole excitations in ^{208}Pb.

E NUCLEAR REACTION ^{208}Pb(d, p), $E = 20$ MeV; measured $\sigma(E_p, \theta)$, deduced Q. ^{209}Pb deduced levels, J, π, S, L. Enriched targets.

1. Introduction

From simple shell-model considerations [1]), the lowest two-particle–one-hole states in ^{209}Pb are expected in the region of 2–3 MeV excitation. This expectation is confirmed by the identification of numerous 2p-1h states in studies of the ^{207}Pb(t, p) and ^{210}Pb(p, d) reactions [2-5]). Detailed calculations [6-9]) imply that a number of these states should be weakly populated in the direct single-neutron transfer reaction, and some evidence for such excitation has been reported [10-12]) in earlier single-neutron stripping investigations, but no systematic studies have been undertaken. As a consequence very little spectroscopic information about the 2p-1h states in ^{209}Pb from single-neutron stripping has been reported.

A number of earlier investigations of the ^{208}Pb(d, p) reaction have concentrated on the strong transitions populating the well-known single-particle states in ^{209}Pb.

† Work supported under USAEC contract AT(11-1)-3074.
†† Present address: Argonne National Laboratory, Argonne, Illinois 60439.
††† Present address: Los Alamos Scientific Laboratory, Los Alamos, New Mexico 87544.

The present measurement was designed to observe the weak transitions to non-single-particle states. Approximately thirty such transitions were identified, populating states between 2.1 and 4.6 MeV excitation in ^{209}Pb. In each case, the proton angular distributions showed the strong forward peaking characteristic of direct reactions. Included among them were transitions to a number of known 2p-1h states. We have assumed that all the weak transitions here reported are, in fact, populating states predominantly 2p-1h in nature; the reaction proceeding through single-particle admixtures in the final state, or via 2p-1h correlations in the target. The hypothesis is reasonable, and is consistent with all the data: it permits a number of interesting conclusions. A considerable amount of new information will be presented about the location and character of 2p-1h states, some of which were not previously identified even in the (p, t) and (p, d) experiments leading to ^{209}Pb. Although 2p-1h states were emphasized in this study, new information about the distribution of single-particle strength in ^{209}Pb was also obtained, particularly with respect to the fragmentation of the $j_{\frac{9}{2}}$ neutron orbital. Finally, from comparison with model calculations it is found that the results of this experiment are consistent with the interpretation that significant departures from shell closures exist in the ^{208}Pb ground state.

In obtaining spectroscopic information from experimental data it is necessary, of course, to understand the reaction process. Because the (d, p) cross sections emphasized in this work are substantially weaker than those normally reported, one must be concerned about the importance of reaction mechanisms more complex than simple one-step transfer. The spins and parities reported for many 2p-1h states in ^{209}Pb based on other reaction studies [2-5]) prove very useful in helping to determine whether the observed transitions are consistent with a simple one-step transfer mechanism, for if the spin and parity of a final state are known, then a one-step transfer of unique l-value is implied. In the present study, not only the angular distributions for the single-particle states, but also those for the weak transitions to the 2p-1h states of known spin and parity are found to have stripping-type patterns. In almost every case, the distributions could be reasonably well fit using standard DWBA calculations with an l-assignment corresponding to the previously known spin and parity of the final state. Although this test by no means eliminates the possibility of more complex processes, it seems reasonable to work with the simplest assumptions until contradictions are reached or until more rigorous calculations of stripping processes including two-step mechanisms become available. Therefore in the following sections the data from this experiment are analyzed assuming a simple one-step reaction process, and angular distributions are compared with results of a conventional DWBA analysis to obtain l-values and spectroscopic factors.

2. Experimental procedure

The experiments were performed with a multigap magnetic spectrograph using 20.0 MeV deuterons obtained from the Yale tandem accelerator. The Yale multigap

spectrograph [13]) consists of 23 broad-range Browne-Buechner spectrographs located at 7.5° intervals around a torus which can be rotated to subtend three angular ranges: 0° to 172.5°, 5.0° to 165.5°, and 8.75° to 163.75°. An energy range of $E_{max}/E_{min} = 2.4$ is spanned by the active focal surface of a single exposure, with a typical solid angle of 3.5×10^{-4} sr. The protons in the present experiment were recorded on nuclear emulsions (Ilford) and scanned by microscope.

The targets consisted of approximately 100 $\mu g/cm^2$ of 99.9 % isotopically pure ^{208}Pb evaporated on 10 $\mu g/cm^2$ carbon foils. The target thickness was established in a separate scattering chamber measurement of the Rutherford cross section at $E_d = 6.0$ MeV using solid-state detectors. Absolute cross sections were determined in the same geometry by measurement of the angular distributions of the elastically scattered deuterons and the proton groups from the (d, p) reaction to the ^{209}Pb single-particle states at $E_d = 20.0$ MeV. Spectrograph data were normalized to these measurements; the absolute cross sections are believed to be established to better than 20 % by this method.

3. Experimental results

Typical proton spectra obtained in this study of the ^{208}Pb(d, p) ^{209}Pb reaction are shown in figs. 1 and 2. In fig. 1 are shown the seven well-known strongly populated single-particle states observed in a short exposure with typical peak cross sections of 1–10 mb/sr. In fig. 2 the weakly populated states (cross sections in the range 10–100 μb/sr) observed in a long exposure are shown in addition to the strong single-particle states. Energy resolution of $\Delta E/E = 0.05$ % (i.e. 10–15 keV) were typical in all spectra. All groups in the spectra were identified either as a ^{209}Pb level or as a contaminant. The ground-state Q-value was measured to be 1.710 ± 0.015 MeV as compared to 1.719 ± 0.014 MeV calculated from known masses [14]).

The energy levels measured up to 5.2 MeV excitation in ^{209}Pb are listed in table 1 where they are compared to the results reported in other studies. In the present study a number of levels are observed which were not reported in previous (d, p) studies. Many of the levels up to 4.5 MeV can be associated with those observed in the ^{210}Pb(p, d)^{209}Pb and ^{207}Pb(t, p)^{209}Pb studies [2–5]) and identified as predominantly of 2p-1h character. Above $E_x = 3.937$ MeV, the levels can also be compared with the results of neutron resonance studies; however, at the higher excitations a definite correspondence between levels reported in different studies becomes less certain because of the higher level densities and the larger errors associated with the energy measurements.

The angular distributions for the strong transitions populating the seven single-particle states are shown in fig. 3. The cross sections at $E_d = 20.0$ MeV were found to be substantially the same as the previous measurements [15]) at 20.3 MeV in all cases except the $2g_{\frac{9}{2}}$ and $1i_{\frac{13}{2}}$ states; these were found to be 20 % and 30 % larger in the present study. The angular distributions for 34 weakly populated levels are shown in figs. 4 and 5. These groups correspond to levels populated in the excitation region

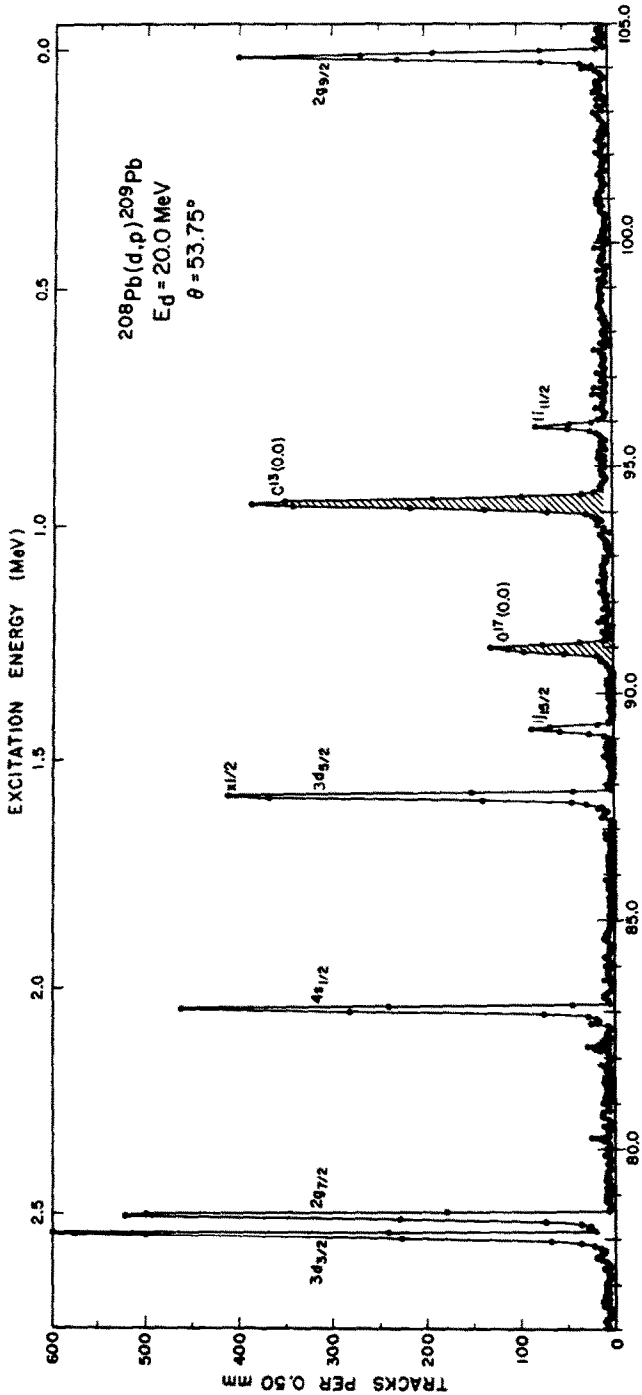

Fig. 1. Typical proton spectrum showing the strongly populated neutron single-particle states in ^{209}Pb obtained in the spectrograph.

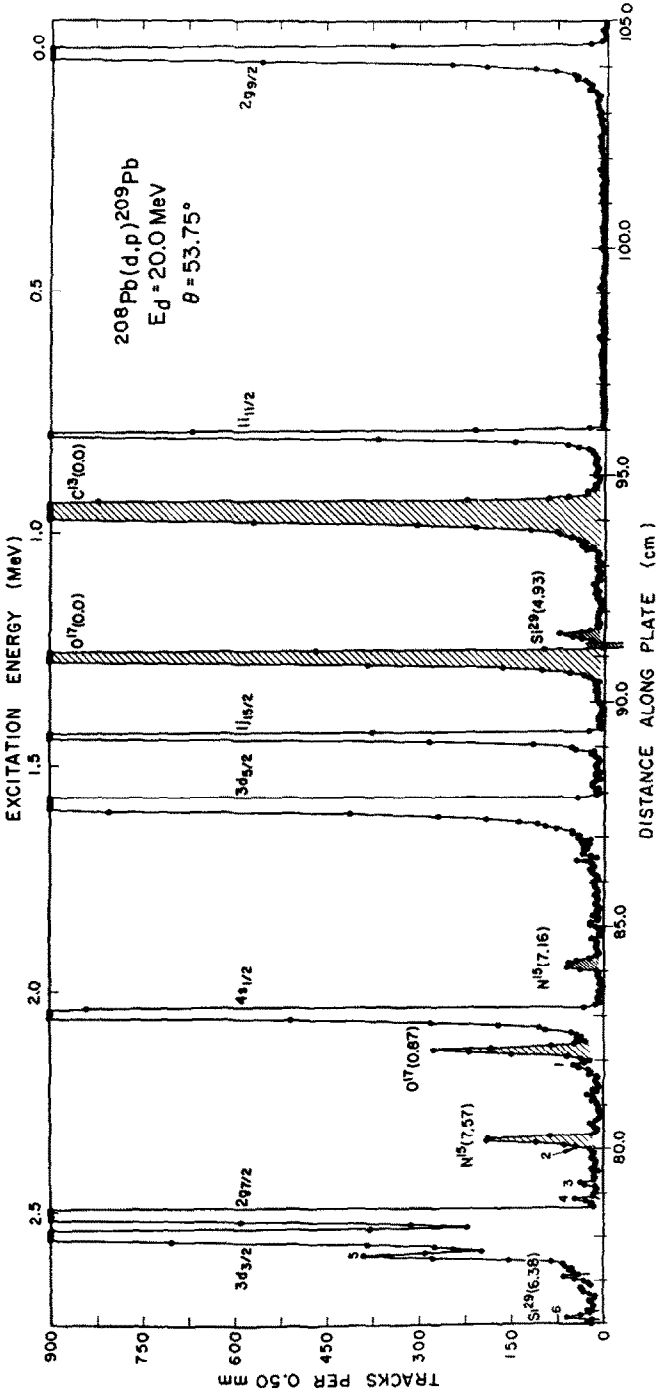
$^{208}Pb(d,p)^{209}Pb$
$E_d = 20.0$ MeV
$\theta = 53.75°$
EXCITATION ENERGY (MeV)
DISTANCE ALONG PLATE (cm)
TRACKS PER 0.50 mm
$2g_{9/2}$
$1i_{11/2}$
$C^{13}(0.0)$
$O^{17}(0.0)$
$Si^{29}(4.93)$
$1i_{13/2}$
$3d_{5/2}$
$4s_{1/2}$
$N^{15}(7.16)$
$O^{17}(0.87)$
$N^{15}(7.57)$
$2g_{7/2}$
$3d_{3/2}$
$Si^{29}(6.38)$

Fig. 2a.

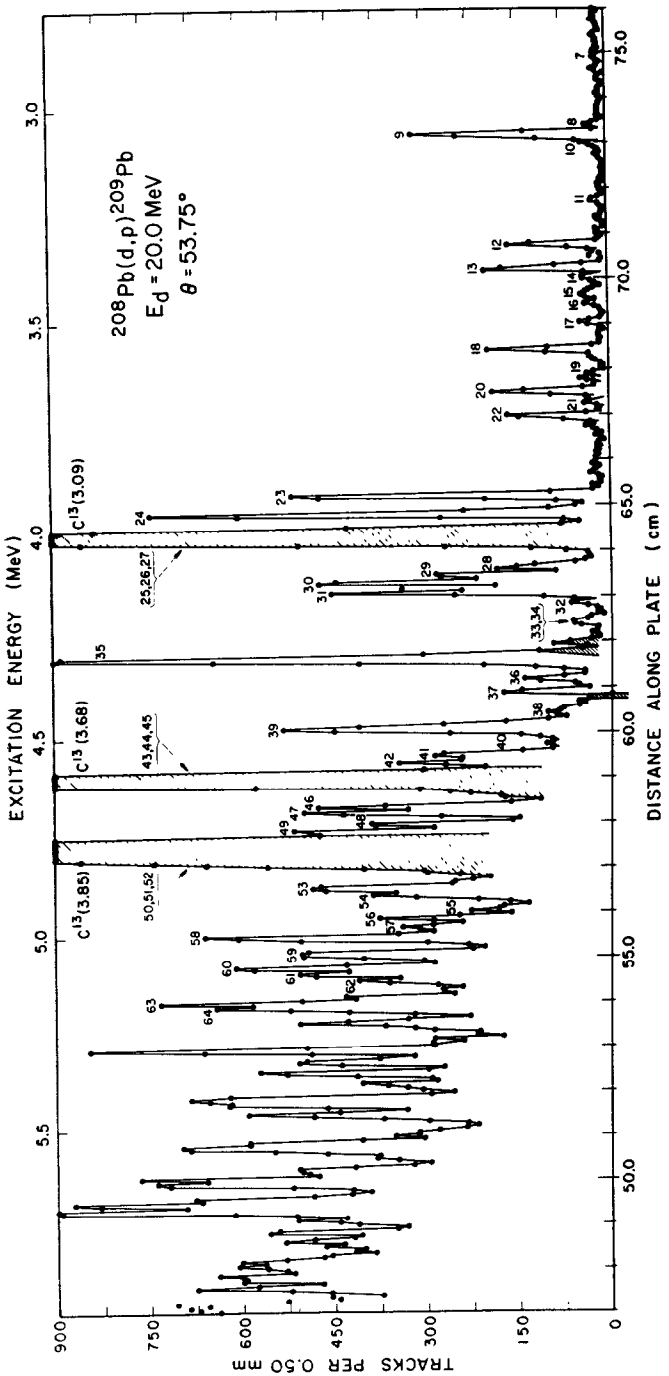

Fig. 2b.

Fig. 2. Weakly populated states observed in the ^{208}Pb(d, p)^{209}Pb reaction in a long spectrograph exposure.

TABLE 1
States in ^{209}Pb

Level no.	Present study (d, p) (MeV)	Previous studies: stripping (d, p)	stripping (t, d) [d]	pick-up (p, d) [c]	two-nucleon transfer (t, p) [f]	neutron [i] studies (n, n′)
$2g_{\frac{9}{2}}$	0.000	0 [c]	0	0	0	
$1i_{\frac{11}{2}}$	0.779±0.005	0.780 [c]	0.781	0.782	0.778 [g]	
$1j_{\frac{15}{2}}$	1.424±0.005	1.424 [c]	1.429	1.426	1.424 [g]	
$3d_{\frac{5}{2}}$	1.565±0.005	1.565 [c]	1.573	1.571	1.568 [g]	
$4s_{\frac{1}{2}}$	2.033±0.005	2.031 [c]	2.039	2.035	2.034 [g]	
1	2.152±0.005	2.155 [a, b]	2.153	2.152	2.152 [g]	
2	2.319±0.005	2.310 [b]		2.320		
3	(2.424)±0.005					
4	2.461±0.005			2.463		
$2g_{\frac{7}{2}}$	2.492±0.005	2.492 [c]	2.496	2.499	2.496	
$3d_{\frac{3}{2}}$	2.537±0.005	2.537 [c]	2.542	2.547	2.542 [g]	
				2.563		
5	2.592±0.005	2.590 [a, b]	2.592	2.584	2.591 [g]	
6	2.738±0.005			2.741	2.737 [g]	
7	2.866±0.005			2.873	2.868 [g]	
				2.906	2.902 [g]	
			2.996		2.992	
8	3.026±0.005			3.031	3.028 [g]	
9	3.052±0.005	3.050 [a, b]	3.049			
10	3.075±0.005			3.077	3.072 [g]	
					3.100	
11	3.203±0.005				3.206 [g]	
12	3.309±0.005	3.310 [a, b]	3.305		3.309 [g]	
13	3.365±0.005	3.368 [a, b]	3.373			
14	3.389±0.005				3.384	
15	3.414±0.005					
16	3.430±0.005				3.432 [g]	
					3.477	
17	3.490±0.005			3.499		
				3.524		
18	3.556±0.005	3.556 [a, b]		3.562	3.561 [g]	
19	3.615±0.005					
20	3.656±0.005	3.656 [a, b]		3.659	3.659	
21	3.681±0.005					
					3.708	
22	3.716±0.005	3.717 [b]				
					3.743	
				3.751		
			3.800	3.811	3.815 [g]	
				3.831		

TABLE 1 (continued)

Level no.	Present study	Previous studies				
		stripping		pick-up	two-nucleon transfer	neutron [1]) studies
	(d, p) (MeV)	(d, p)	(t, d) [d])	(p, d) [e])	(t, p) [f])	(n, n′)
					3.854	
23	3.904±0.005	3.905 [a, b])		3.906	3.902	
				3.937		
24	3.947±0.005	3.948 [a, b])			3.946	
25	3.985±0.005	3.985 [a])	3.990			
				3.995	3.992 [g])	
26	4.008±0.005	4.010 [a, b])				4.014 [h, i])
27	4.022±0.005	4.021 [a, b])		4.024	4.022	4.028 [i])
						4.056 [h])
28	4.075±0.005	4.075 [a])	4.075		4.074	
				4.084		
29	4.096±0.005	4.095 [a])	4.094		4.100 [g])	4.100 [h, i])
30	4.112±0.005	4.113 [a, b])		4.119		
31	4.137±0.005	4.138 [a, b])	4.146	4.145	4.140	
32	4.166±0.005	4.175 [b])		4.174	4.169	
33	4.211±0.007	4.216 [a])		4.212		4.215 [h])
34	(4.239)±0.010			4.222		
				4.270	4.260 [g])	
					4.289	4.289 [h, j])
35	4.295±0.005	4.298 [a, b])	4.283			
				4.309		
			4.322		4.315	
36	4.348±0.005	4.350 [a])		4.345		4.344 [h])
				4.358	4.361 [g])	
37	4.380±0.005				4.384	
				4.395		
		4.415 [b])			4.413	
38	4.430±0.009					4.426 [h])
						4.441 [h])
39	4.464±0.007				4.451 [g])	4.463 [h, j])
				4.472		
40	4.502±0.010	4.501 [b])			4.508	4.500 [h])
41	4.530±0.010			4.529		
					4.542 [g])	
42	4.552±0.010			4.562		
43	4.575±0.010			4.584	4.578	4.573 [h])
44	4.612±0.010					
45	4.629±0.010			4.621	4.632 [g])	4.623 [h])
						4.638 [h])
46	4.661±0.010				4.660	4.660 [h, j, k])
47	4.676±0.010			4.671		
				4.690	4.686	

TABLE 1 (continued)

Level no.	Present study	Previous studies				
		stripping		pick-up	two-nucleon transfer	neutron [l]) studies
	(d, p) (MeV)	(d, p)	(t, d) [d]	(p, d) [e]	(t, p) [f]	(n, n')
48	4.706±0.010			4.715	4.715	4.706 [k])
49	4.726±0.010				4.731	
50	4.747±0.010				4.743	
					4.754	4.758 [k])
51	4.764±0.010					
				4.781	4.778	
52	4.799±0.010					4.792 [k])
				4.819	4.813	
				4.837	4.843	
53	4.864±0.010			4.865	4.877	
54	4.885±0.010				4.904	4.890 [k])
55	4.920±0.010			4.924	4.931	
56	4.940±0.010			4.944		
57	4.962±0.010				4.966	
58	4.986±0.010				4.997	
59	5.028±0.010				5.026	
						5.049 [k])
60	5.061±0.010				5.057	
61	5.085±0.010			5.074	5.083	5.091 [k])
62	5.102±0.010			5.094	5.107	
			5.136	5.136	5.134	5.141 [k])
63	5.153±0.010			5.160	5.161	
64	5.170±0.010					5.176 [k])
				5.222	5.211	5.222 [k])
						5.291 [k])
					5.326	5.323 [k])
					5.341	
				5.359		5.368 [k])
					5.400	5.414 [k])
					5.423	
					5.476	
					5.513	
						5.537 [k])
					5.577	5.569 [k])
					5.600	
					5.637	5.638 [k])

[a]) Ref. [10]).
[b]) Ref. [11]).
[c]) Many references including [10, 11, 15]).
[d]) Ref. [12]).
[e]) Refs. [2, 3]).
[f]) Refs. [2, 4]).
[g]) Ref. [5]).
[h]) Ref. [37]).
[i]) Ref. [38]).
[j]) Ref. [39]).
[k]) Ref. [40]).
[l]) S_n(209) taken to be 3.937±0.010 MeV (Nuclear Data Sheets 1963).

The level numbers refer to states seen in the ^{208}Pb(d, p)^{209}Pb reaction (see fig. 2).

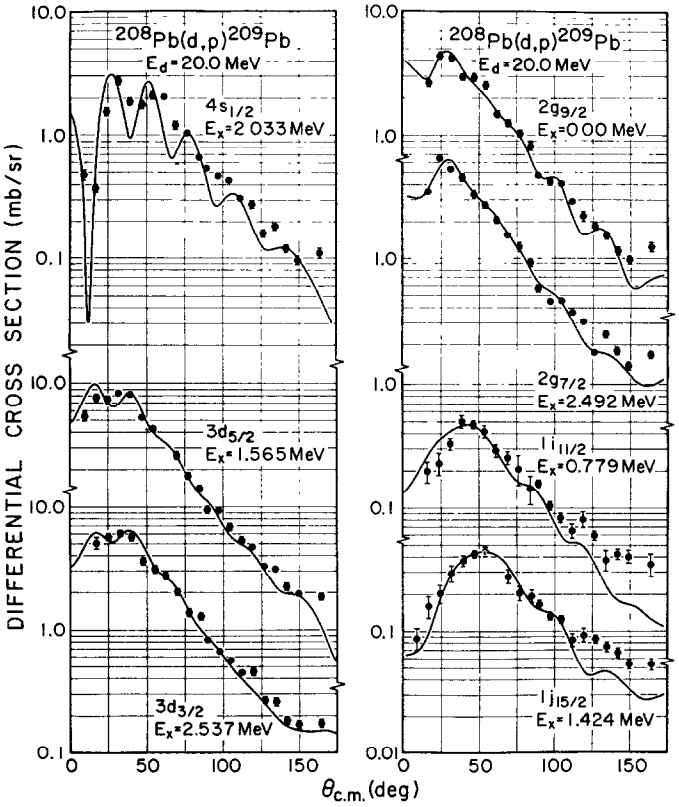

Fig. 3. Angular distributions observed for the transitions to the seven specified single-particle states in ^{209}Pb. The solid curves are DWBA fits.

2.0 to 4.5 MeV in ^{209}Pb. The curves drawn in the figures represent the results of the DWBA calculations to be discussed in the next section.

4. DWBA analysis of angular distributions

4.1. METHOD OF ANALYSIS

4.1.1. General considerations. The experimental data were analyzed with the distorted wave Born approximation (DWBA) code DWUCK [16]). The distorted waves were generated by optical-model potentials derived from fits to elastic scattering data. The bound-state form factors were generated as eigenfunctions of a Woods-Saxon well using the separation-energy prescription [17,18]). The cross section for the (d, p) reaction on a spin zero target can be written in the framework of the zero-range local approximation (ZRL) as [16,18])

$$\mathrm{d}\sigma/\mathrm{d}\Omega = N_0 S_{lj} \sigma_{lj}^{\mathrm{DW}}(\theta),$$

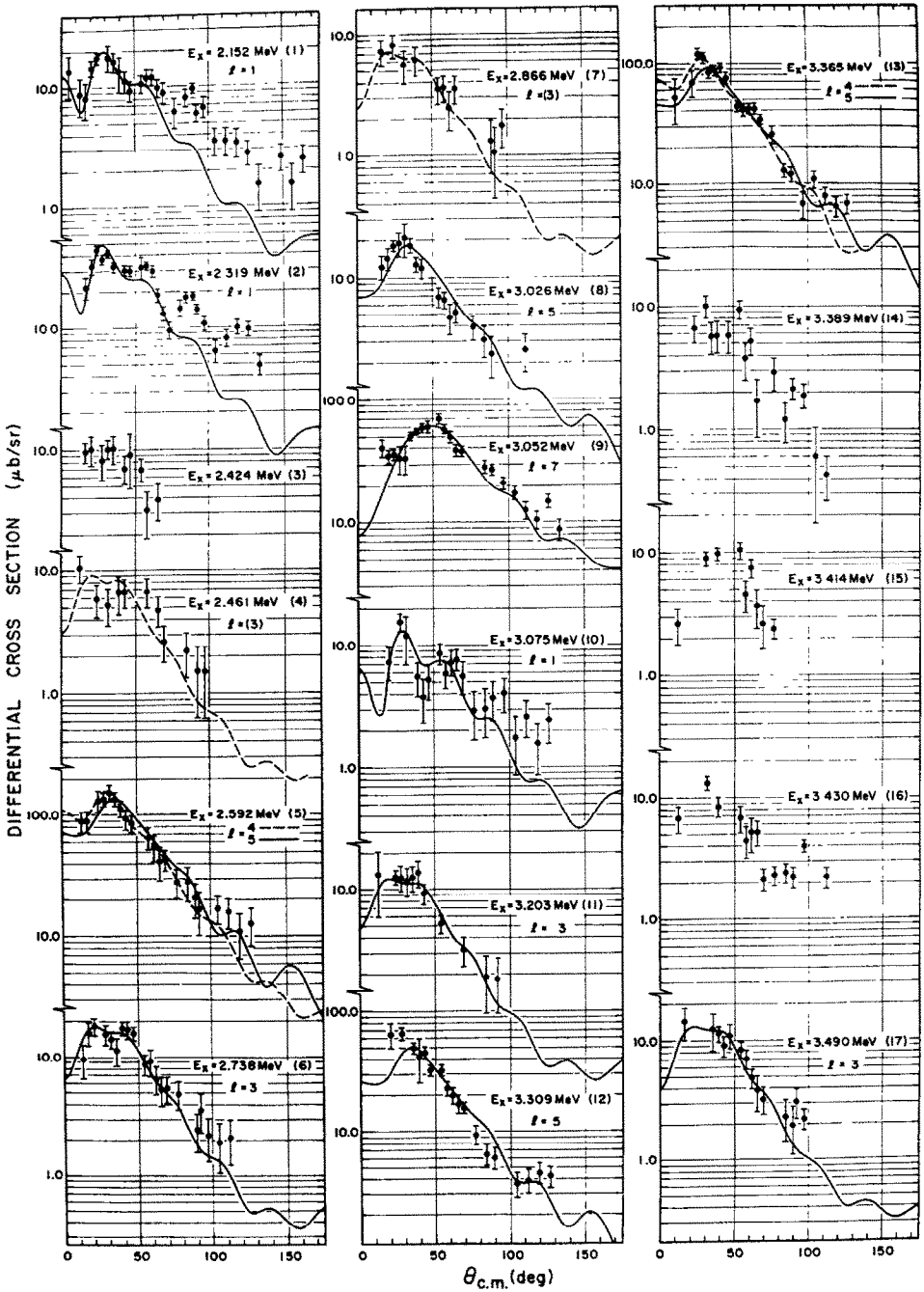

Fig. 4. Angular distributions of the weak transitions for levels 1 through 17 observed in the excitation region 2.1–3.5 MeV in ^{209}Pb. The solid curves are DWBA fits. The dashed curves are tentative fits.

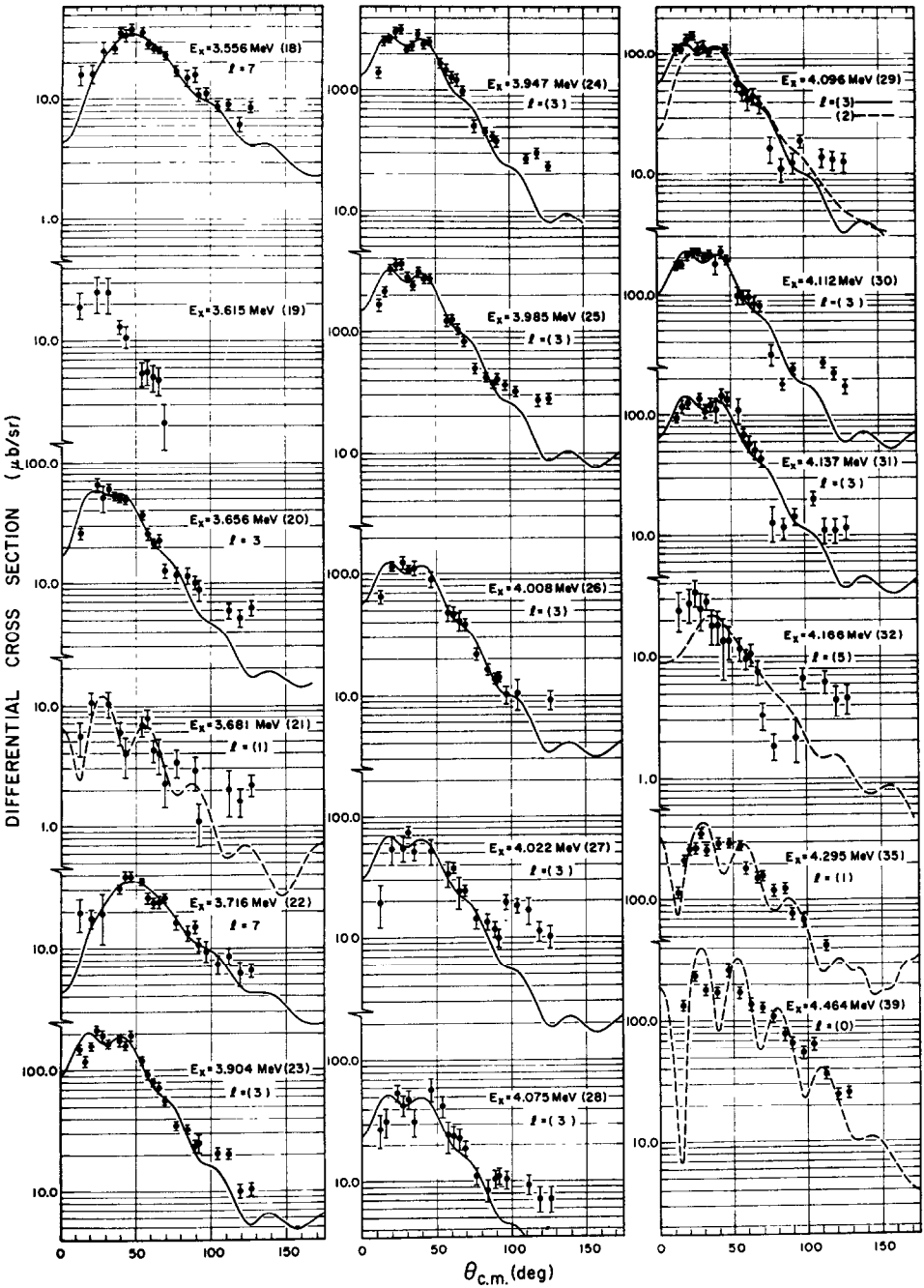

Fig. 5. Angular distributions of the weak transitions for levels 18 through 32, 35 and 39 observed in the excitation region 3.5–4.5 MeV. The solid curves are DWBA fits. The dashed curves are tentative fits.

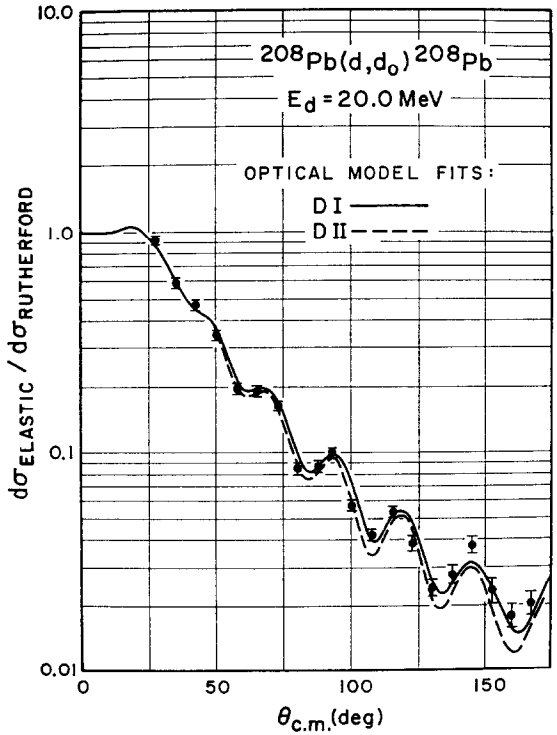

Fig. 6. Optical-model fits to the measured deuteron elastic cross section. Parameter set DI was obtained from a search of the data. Parameter set DII is taken from the literature [20]).

where N_0 is the zero-range normalization factor taken here to be 1.5, $\sigma_{lj}^{DW}(\theta)$ is the cross section calculated by DWUCK for the orbital lj, and S_{lj} is the spectroscopic factor.

4.1.2. Optical-model parameters. The deuteron optical potential was determined from fitting of 20.0 MeV elastic cross sections measured in this study. A least square fit to the data was made using the search program ABACUS-II [19]) starting with a parameter set obtained in an analysis of 21.5 MeV deuteron elastic scattering from Pb by Satchler [20]). The fits obtained to the present elastic data using the Satchler parameters and those determined from the search are shown in fig. 6 (denoted as DII and DI, respectively), where it is shown that except for the largest angles they are essentially identical. Since the Satchler parameter set had been used in previous analyses of data at these energies [15]), it was decided to use it in the present case also; the parameters are listed in table 2.

The proton optical potential used in the present analysis is based on one proposed for 17.0 MeV protons [21]) on Pb and found to give good fits to cross sections and polarizations for protons of 19, 20, 25 and 30 MeV scattered from Pb [ref. [22])]. The parameter set is listed in table 2. No spin-orbit terms were used in the potentials for the protons or deuterons.

TABLE 2

Optical-model and bound-state parameters used in distorted-wave calculations

Parameter set	V (MeV)	r_0 (fm)	a_0 (fm)	W (MeV)	W_D (MeV)	r_0' (fm)	a_0' (fm)	r_c (fm)
deuterons	100.0	1.14	0.89	0	13.80	1.33	0.75	1.30
protons	52.0	1.25	0.65	0	10.0	1.25	0.76	1.25
neutrons	V_n [a])	1.23	0.65	($\lambda = 25$)[b])				
deuteron (break-up)	112	1.25	0.682	0	19.4	1.25	0.783	1.30

Also listed is the deuteron-breakup potential discussed in the text.

[a]) Adjusted to give binding energy equal to separation energy.

[b]) Spin-orbit coupling of λ times the Thomas term.

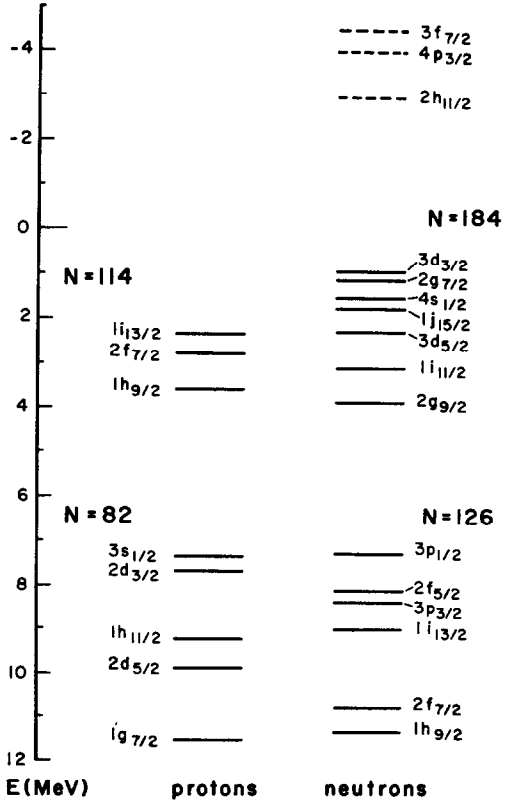

Fig. 7. Predicted ordering of the proton and neutron shell-model orbits in the mass region $A = 208$.

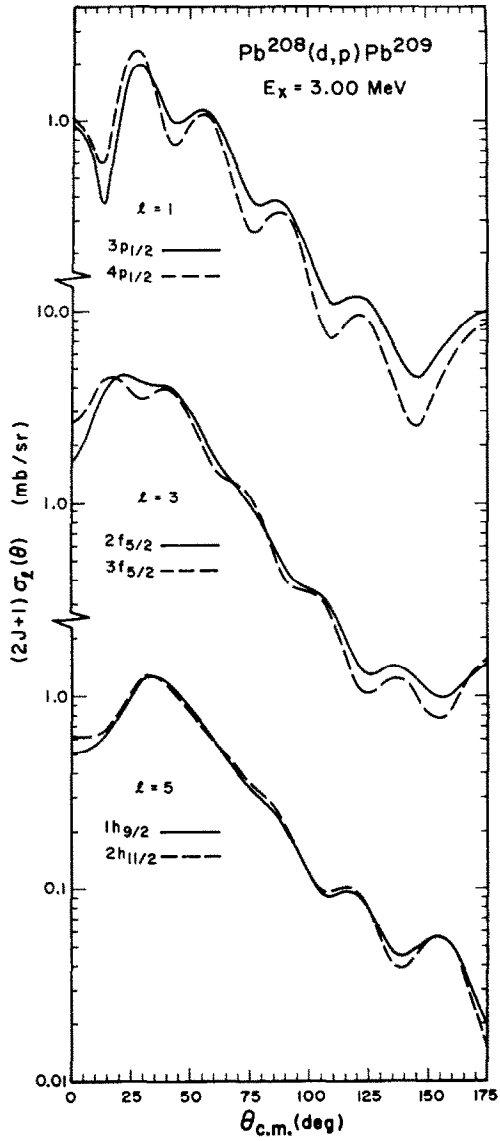

Fig. 8. Comparison of DWBA curves calculated for stripping into shell-model orbits of similar l, but different radial quantum number n. The normalizations are adjusted to illustrate the similarity in shapes.

4.1.3. Neutron form factors. The neutron form factors used in the analysis of the stripping cross sections were calculated using the separation-energy prescription with bound-state well parameters $r_0 = 1.23$ fm, $a = 0.65$ fm, and $\lambda = 25$ obtained from sub-Coulomb stripping [23]). While there exist some questions concerning the exact values of parameters to employ for the bound-state potential [24]), the use of the

separation-energy prescription in the analysis of the strong transfers to the single-particle states is quite reasonable [25,26]). Their analysis was used primarily as a "calibration" to limit the ambiguities in the DWBA analysis of the weaker transfers. For the weak transfers the use of the separation prescription appears to be a rather poor approximation. Essentially all the 2p-1h states in the excitation region studied are expected to be of negative parity and hence must be populated by an odd-l transfer. Since the major neutron shell (N = 126–184 neutrons) is composed of positive-parity orbits (except for the $1j_{\frac{15}{2}}$ orbit) the stripping must proceed into orbits of the adjacent shells; i.e. the shell N = 82–126 neutrons, corresponding to the orbits below the Fermi level, or the shell $N > 184$ neutrons, corresponding to the unbound orbits of ^{209}Pb (see fig. 7). This makes it possible to populate a final state by stripping a neutron into one (or both) of two shell-model orbitals of the same lj, but different radial quantum number n. In fig. 8 are shown the predicted (ZRL) DWBA cross sections for the transfers of l = 1, 3, and 5 leading to orbits with similar quantum numbers lj, but different radial quantum number n. The shapes are, to a great extent, similar and recognizable despite the fact they are several MeV displaced from their centroid position. The cross sections for the transfers into the orbit with larger n were found to be uniformly about a factor of 2 greater than that predicted for the orbit of smaller n. (The transfer cross sections for orbits of different radial quantum number in fig. 8 have been adjusted to illustrate the similarity in shapes.) For either value of n, the transition corresponds to stripping to a final state via a single-particle component at some distance from its centroid position, a situation in which there is doubt about the accuracy of the form factor calculated using the separation energy [5–8]). Some realistic form factor calculations have been reported and their results have been compared to those obtained using the conventional prescription [25–28]). It was found that while the predicted angular distributions have very similar shapes, the magnitude of the predicted cross sections, in the examples studied, differed by as much as a factor of 2 to 4. Thus, though it appears to be possible to assign l-values from an analysis using the separation-energy prescription, the spectroscopic factors must be considered uncertain by a factor of 2 or more.

4.2. RESULTS OF DWBA ANALYSIS

4.2.1. Single-particle states. The theoretical DWBA angular distributions are compared in fig. 3 with the experimental data for the strong single-particle states in ^{209}Pb. The quality of the fits is similar to what has been found in previous studies of this reaction at these energies [15]). In general, the basic shapes of the angular distributions are fitted, but the finer details are not always well reproduced. The greatest difficulty appears to be in reproducing the sharp oscillatory structure associated with the $4s_{\frac{1}{2}}$ state.

The spectroscopic factors obtained for the single-particle states are listed in table 3 where they are compared with the results from previous studies in which similar analyses were employed [10–12,23]). The spectroscopic factors from the present study

TABLE 3

Comparison of spectroscopic factors for the ^{209}Pb single-particle states obtained in studies at different bombarding energies from analyses using ZRL DWBA

nlj	Dost and Herring [a])	Oxford [b]) (8 MeV)	Copenhagen [c]) (12 MeV)	Oxford [b]) (18.7 MeV)	Los Alamos [d]) (t, d) (20.0 MeV)	This study (20.0 MeV)
$2g_{\frac{9}{2}}$	1.07	1.04	0.78±0.1	0.66	0.76	0.83 (0.92) [e])
$1i_{\frac{11}{2}}$		1.07	0.96±0.2	0.75	0.86	0.86 (1.14)
$1j_{\frac{15}{2}}$			0.53±0.2	0.71	0.49	0.58 (0.77)
$3d_{\frac{5}{2}}$	1.14	0.98	0.88±0.1	0.62	0.84	0.98 (0.89)
$4s_{\frac{1}{2}}$	1.11	0.96	0.88±0.1	0.70	0.82	0.98 (0.85)
$2g_{\frac{7}{2}}$	0.98	1.03	0.78±0.1	0.81	0.86	1.05 (0.95)
$3d_{\frac{3}{2}}$	1.01	0.98	0.88±0.1	0.88	0.79	1.07 (0.99)

Spectroscopic factors obtained from analysis with the deuteron-breakup potential are listed in the last column.

[a]) Ref. [23]).
[b]) Ref. [11]).
[c]) Ref. [10]).
[d]) Ref. [12]).
[e]) Using deuteron break-up potential.

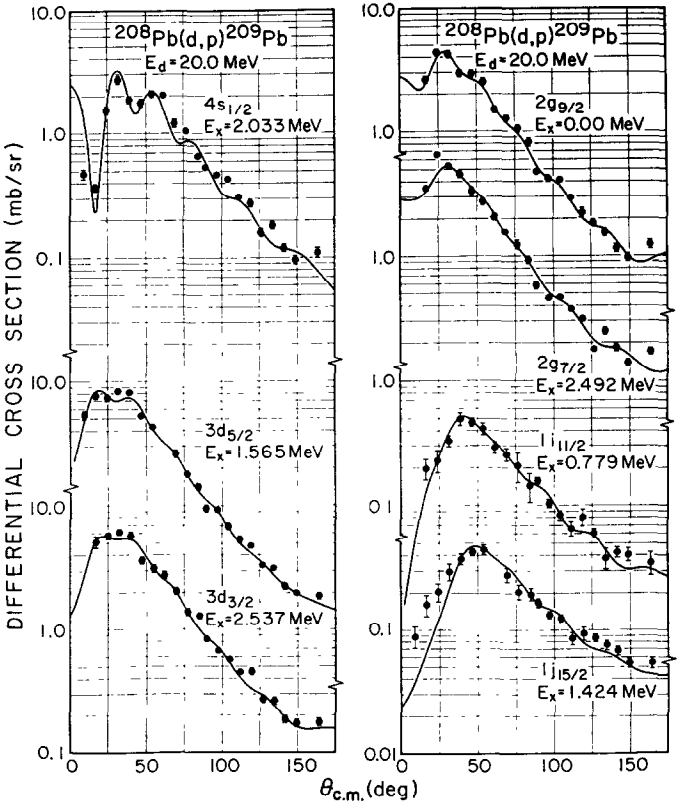

Fig. 9. Fits to the transfers populating the seven single-particle states by DWBA calculations using the deuteron break-up potential (see table 2).

all lie within $\approx 20\,\%$ of unity except for the $1j_{\frac{9}{2}}$ state at 1.424 MeV with a spectroscopic factor of 0.58. These results agree with the relative spectroscopic factors obtained in the (t, d) work at 20 MeV and the (d, p) work at 12 MeV. In the early work on ^{209}Pb, it had been assumed that the 1.424 MeV state exhausted the $1j_{\frac{9}{2}}$ strength but the present study confirms the more recent work in which only 50–70 % of the strength is found in that state.

The effects caused by the variation of the optical-model and bound-state parameters, and by the inclusion of finite-range and nonlocality corrections in the DWBA have been discussed in the literature [11, 15]). Similar results were obtained in our investigation of these effects [29]) and they will not be discussed here. Recently, however, Soper and Johnson [30]) proposed the use of an effective deuteron optical-model potential to include approximately the contributions from deuteron breakup. DWBA fits to the present data in which the deuteron breakup potential was used are shown in fig. 9. The optical-model parameters used in the analysis are the same as those used by Satchler [22]) in his analysis of the ^{208}Pb(p, d)^{207}Pb reaction [31]) and are listed in table 2. These results show a decided improvement in some of the fits to the data. The spectroscopic factors obtained using the deuteron breakup potential are listed in table 3 and compared with those based on the conventional deuteron potential. Differences of the order of 10 % for the small-l transfer and up to 30 % for the large-l transfers are observed. Further inclusion of finite-range and nonlocality corrections make essentially no change in either the fits to the data or the spectroscopic factors.

4.2.2 Two-particle–one-hole states. The experimental angular distributions and the zero-range DWBA fits to the data for 34 weak transitions measured in this experiment are shown in figs. 4, 5. Calculations were also performed with the deuteron breakup potential and the effects proved to be similar to what was found in the case of the strong transitions; namely, the predicted oscillations were damped (with no improvement in the fits in this case), and the spectroscopic factors were modified by 10–20 %. In view of the much larger uncertainties associated with the form factors for the weaker transitions, the effects due to the deuteron potential appear to be small and the results for the weak transition presented here are based on conventional parameters.

In the usual picture of a single-nucleon stripping reaction, the final state is populated by stripping into an orbital specified by quantum numbers nlj. As mentioned earlier, it is possible in principle to populate a 2p-1h state by stripping into two orbits of similar lj, but different radial quantum number n. In our analysis we assumed the reaction could proceed via either one or the other of the two orbits and determined spectroscopic factors for each. The DWBA curves for only one of the orbits are shown in figs. 4, 5 since the predicted curves were shown in fig. 8 to have basically the same shape. The solid curves in figs. 4, 5 are calculations corresponding to the indicated l-assignments. The dashed curves imply tentative l-assignments unless otherwise noted. They represent less certain fits to the data, or, in several cases assignments which would not necessarily have been made on the basis of the data alone, but which are consistent with the data and with information from other studies.

The overall conclusion implied by the angular distributions for the 34 2p-1h states shown in figs. 4, 5 is that the reaction mechanism is a direct one. It was by no means obvious before performing this experiment that so many of the weak transitions would result in stripping type angular distributions as the data in figs. 4, 5 appear to indicate. Though there are a few poor fits, in general the DWBA calculations are able to reproduce the angular distributions rather well. The $l = 1$ transitions are rather distinctive and relatively easy to identify because of their maxima at about 25° and 60°. The large-l transfers (i.e. $l = 6$ and 7) are also distinctive by virtue of the peak in their angular distributions at relatively large angles and their slowly decreasing cross sections at large angles. The $l = 6$ and 7 transfers are dissimilar enough to be distinguished from each other. It was not possible, however, to distinguish between $l = 2$ and 3 and between $l = 4$ and 5 transfers on the basis of fitting angular distributions. It was assumed that the l-transfers to states below about 4.0 MeV must be odd-l transfers based on simple shell-model and weak coupling arguments, i.e. that except for the $(^{210}\mathrm{Pb}(0^+)_{\mathrm{g.s.}} \otimes \mathrm{i}_{\frac{13}{2}}^{-1})$ state there should be no positive-parity 2p-1h states below 4.0 MeV excitation. These arguments are supported by more sophisticated model calculations [7]) and by the results of experimental studies [3,4]).

Neutron bound states. Table 4 contains the l-value and j-assignments for the 2p-1h states measured in the present experiment up to the neutron binding energy of 3.937 MeV. They are compared with similar information obtained in the studies [3,4]) of the $^{210}\mathrm{Pb(p, d)}^{209}\mathrm{Pb}$ and $^{207}\mathrm{Pb(t, p)}^{209}\mathrm{Pb}$ reactions. In the case of the (p, d) study [3]) 2p-1h configurations of the form $(^{210}\mathrm{Pb}(0^+)_{\mathrm{g.s.}} \otimes lj^{-1})$ are populated; tentative lj assignments based on sum rules have been placed in parentheses. In the (t, p) reaction on ^{207}Pb, 2p-1h configurations of the form $(^{210}\mathrm{Pb}(\lambda^\pi) \otimes \mathrm{p}_{\frac{1}{2}}^{-1})_{J=\lambda\pm\frac{1}{2}}$ are strongly populated, where the spin and parity λ^π are given uniquely by the L-transfer and $J = L \pm \frac{1}{2}$. By their nature, both of these reactions should provide reliable information concerning the 2p-1h structure in ^{209}Pb, and thus comparison with assignments based on the present experiment is extremely important in establishing the validity of the interpretation of the weak transitions in the (d, p) reaction as populating 2p-1h states. As can be seen in table 4, roughly two-thirds of the levels observed in the 2p-1h reactions are also observed in the (d, p) reaction, and in addition almost every l-assignment based on the (d, p) transition agrees with the information based on the 2p-1h reactions where such information exists. Based on this evidence for the reliability of the present l-assignments, they can be used to resolve some of the spin assignments which were left ambiguous by previously available information, and also to identify levels not assigned or reported previously. The last column in table 4 lists the most probable J^π assignments for the levels observed in ^{209}Pb based on all the presently available information.

Neutron unbound states. Angular distributions for the first eight levels above the neutron binding energy in the excitation region 3.940 MeV to 4.140 MeV were found to be very similar and could be reasonably well fit as either $l = 2$ or $l = 3$ transfers (see fig. 5). The cross sections calculated for the transfers to the neutron

TABLE 4

J^π information from transfer reaction studies for the *bound* states in ^{209}Pb

Level no.	E_x (MeV)	Previous work				Present work		Most probable J^π
		^{210}Pb(p, d)^{209}Pb[a]		^{207}Pb(t, p)^{209}Pb[b]		^{208}Pb(d, p)^{209}Pb		
		l	J^π	L	J^π	l	J^π	
1	2.152	1	$\frac{1}{2}^-$	0	$\frac{1}{2}^-$	1	$(\frac{1}{2}^-, \frac{3}{2}^-)$	$\frac{1}{2}^-$
2	2.319	1	$(\frac{3}{2}^-)$			1	$(\frac{1}{2}^-, \frac{3}{2}^-)$	$\frac{3}{2}^-$
3	(2.424)					*		
4	2.461	3	$(\frac{5}{2}^-)$			(3)	$(\frac{5}{2}^-, \frac{7}{2}^-)$	$(\frac{5}{2}^-)$
	2.563[a]	3	$(\frac{5}{2}^-, \frac{7}{2}^-)$					$(\frac{5}{2}^-, \frac{7}{2}^-)$
5	2.592	*		*		5[c]	$(\frac{9}{2}^-, \frac{11}{2}^-)$	$(\frac{11}{2}^-)$
6	2.738	3	$\frac{5}{2}^-$	2	$(\frac{3}{2}^-, \frac{5}{2}^-)$	3	$(\frac{5}{2}^-, \frac{7}{2}^-)$	$\frac{5}{2}^-$
7	2.866	3	$\frac{5}{2}^-$	2	$(\frac{3}{2}^-, \frac{5}{2}^-)$	(3)	$(\frac{5}{2}^-, \frac{7}{2}^-)$	$\frac{5}{2}^-$
	2.906[a]	1	$\frac{3}{2}^-$	2	$(\frac{3}{2}^-, \frac{5}{2}^-)$			$\frac{3}{2}^-$
	2.992[b]			2	$(\frac{3}{2}^-, \frac{5}{2}^-)$	*[d]		$(\frac{3}{2}^-, \frac{5}{2}^-)$
8	3.026	1	$(\frac{3}{2}^-)$	4	$(\frac{7}{2}^-, \frac{9}{2}^-)$	5	$(\frac{9}{2}^-, \frac{11}{2}^-)$	$(\frac{3}{2}^-)$, $(\frac{9}{2}^-)$ †
9	3.052					7	$(\frac{13}{2}^-, \frac{15}{2}^-)$	$\frac{15}{2}^-$
10	3.075	(1)	$(\frac{3}{2}^-)$	6	$(\frac{11}{2}^-, \frac{13}{2}^-)$	1	$(\frac{1}{2}^-, \frac{3}{2}^-)$	$(\frac{3}{2}^-)$, $(\frac{13}{2}^-)$ †
	3.100			8	$(\frac{15}{2}^-, \frac{17}{2}^-)$			$(\frac{15}{2}^-, \frac{17}{2}^-)$
11	3.203			4	$(\frac{7}{2}^-, \frac{9}{2}^-)$	3	$(\frac{5}{2}^-, \frac{7}{2}^-)$	$\frac{7}{2}^-$
12	3.309			6	$(\frac{11}{2}^-, \frac{13}{2}^-)$	5	$(\frac{9}{2}^-, \frac{11}{2}^-)$	$\frac{11}{2}^-$
13	3.365					5	$(\frac{9}{2}^-, \frac{11}{2}^-)$	$(\frac{11}{2}^-)$
14	3.389			*				
15	3.414					*		
16	3.430			8	$(\frac{15}{2}^-, \frac{17}{2}^-)$	*	††	$(\frac{15}{2}^-, \frac{17}{2}^-)$
	3.477[b]			*				
17	3.490	3	$(\frac{7}{2}^-)$			3	$(\frac{5}{2}^-, \frac{7}{2}^-)$	$\frac{7}{2}^-$
	3.524[a]	(1)	$(\frac{3}{2}^-)$					$(\frac{3}{2}^-)$
18	3.556	(1)	$(\frac{3}{2}^-)$	8	$(\frac{15}{2}^-, \frac{17}{2}^-)$	7	$(\frac{13}{2}^-, \frac{15}{2}^-)$	$\frac{15}{2}^-$, $(\frac{3}{2}^-)$ †
19	3.615					*		
	3.637[a]	(1)	$(\frac{3}{2}^-)$					$(\frac{3}{2}^-)$
20	3.656	6	$\frac{13}{2}^+$	2	$(\frac{3}{2}^-, \frac{5}{2}^-)$	3	$(\frac{5}{2}^-, \frac{7}{2}^-)$	$\frac{6}{2}^-$, $\frac{13}{2}^+$ †
21	3.681					(1)	$(\frac{1}{2}^-, \frac{3}{2}^-)$	$(\frac{1}{2}^-, \frac{3}{2}^-)$
	3.708[b]			3	$(\frac{5}{2}^+, \frac{7}{2}^+)$			$(\frac{5}{2}^+, \frac{7}{2}^+)$
22	3.716					7	$(\frac{13}{2}^-, \frac{15}{2}^-)$	$\frac{15}{2}^-$
	3.743[b]			4	$(\frac{7}{2}^-, \frac{9}{2}^-)$			$(\frac{7}{2}^-, \frac{9}{2}^-)$
	3.751[a]	(6)	$(\frac{13}{2}^+)$					$(\frac{13}{2}^+)$
	3.811[a]	(6)	$(\frac{13}{2}^+)$	*				$(\frac{13}{2}^+)$
	3.831[a]	(1)	$(\frac{3}{2}^-)$					$(\frac{3}{2}^-)$
	3.854[b]			*				
23	3.904	(3)	$(\frac{7}{2}^-)$	*		3	$(\frac{5}{2}^-, \frac{7}{2}^-)$	$(\frac{7}{2}^-)$

Most probable J^π assignments are listed in the last column.

[a]) Ref. [3]).

[b]) Ref. [4]).

[c]) Ref. [10]).

[d]) Ref. [12]).

* Level observed.

† Closely spaced doublet.

†† Small J-value indicated from angular distribution.

unbound states were computed with form factors bound by 100 keV. Two other transfers leading to states at 4.295 MeV and 4.464 MeV appear to correspond to either $l = 0$ or $l = 1$ transfers. The only other angular distribution that could be measured in the neutron unbound region of the spectra corresponds to the level at 4.166 MeV with a possible $l = 5$ assignment in agreement with the $L = 6$ transition assigned in the (t, p) study. All the transitions in the unbound region were measured to have cross sections which were factors of 2 to 10 times larger than those observed for the 2p-1h states at lower excitation.

TABLE 5

J^π information obtained from transfer reaction studies for neutron unbound states of ^{209}Pb

Level no.	E_x (MeV)	Previous work				Present work		Most probable J^π
		^{210}Pb(p,d)^{209}Pb[a]		^{207}Pb(t,p)^{209}Pb[b]		^{208}Pb(d,p)^{209}Pb		
		l	J^π	L	J^π	l	J^π	
	3.937 [a]	6	$(\frac{13}{2}^+)$					$(\frac{13}{2}^+)$
24	3.947			*		(2, 3)	$(\frac{3}{2}^+, \frac{5}{2}^\pm, \frac{7}{2}^-)$	$(\frac{7}{2}^-)$ †
25	3.985					(2, 3)	$(\frac{3}{2}^+, \frac{5}{2}^\pm, \frac{7}{2}^-)$	$(\frac{7}{2}^-)$ †
	3.995 [a]	6	$(\frac{13}{2}^+)$	*				$(\frac{13}{2}^+)$
26	4.008					(2, 3)	$(\frac{3}{2}^+, \frac{5}{2}^\pm, \frac{7}{2}^-)$	$(\frac{7}{2}^-)$ †
27	4.022	(1)	$(\frac{3}{2}^-)$	4	$(\frac{7}{2}^-, \frac{9}{2}^-)$	(2, 3)	$(\frac{3}{2}^+, \frac{5}{2}^\pm, \frac{7}{2}^-)$	$(\frac{3}{2}^-)$, $(\frac{7}{2}^-)$ ††
	4.056 [c]							
28	4.075			*		(2, 3)	$(\frac{3}{2}^+, \frac{5}{2}^\pm, \frac{7}{2}^-)$	$(\frac{7}{2}^-)$ †
	4.084 [a]	(1)	$(\frac{3}{2}^-)$					
29	4.096			3	$(\frac{5}{2}^+, \frac{7}{2}^+)$	(2, 3)	$(\frac{3}{2}^+, \frac{5}{2}^\pm, \frac{7}{2}^-)$	$(\frac{5}{2}^+)$
30	4.112	1	$(\frac{3}{2}^-)$			(2, 3)	$(\frac{3}{2}^+, \frac{5}{2}^\pm, \frac{7}{2}^-)$	$(\frac{3}{2}^-, (\frac{7}{2}^-)$ †,††
31	4.137	*		*		(2, 3)	$(\frac{3}{2}^+, \frac{5}{2}^\pm, \frac{7}{2}^-)$	$(\frac{7}{2}^-)$ †
32	4.166	*		6	$(\frac{11}{2}^-, \frac{13}{2}^-)$	(5)	$(\frac{9}{2}^-, \frac{11}{2}^-)$	$(\frac{11}{2}^-)$
33	4.211	(3)	$(\frac{7}{2}^-)$			*		$(\frac{7}{2}^-)$
(34)	4.222 [a]	3	$(\frac{7}{2}^-)$			*		$(\frac{7}{2}^-)$
	4.270 [a]	3	$(\frac{7}{2}^-)$	*				$(\frac{7}{2}^-)$
	4.289 [b]			*				
35	4.295					((0, 1))	$(\frac{1}{2}^\pm, \frac{3}{2}^-)$	$((\frac{3}{2}^-))$ †
	4.309 [a]	3	$(\frac{7}{2}^-)$					$(\frac{7}{2}^-)$
	4.315 [b]			*				
36	4.348	*						
	4.361 [b]	*		2	$(\frac{3}{2}^-, \frac{5}{2}^-)$			$(\frac{3}{2}^-, \frac{5}{2}^-)$
37	4.380			6	$(\frac{11}{2}^-, \frac{13}{2}^-)$	*		$(\frac{11}{2}^-, \frac{13}{2}^-)$
	4.395 [a]	3	$(\frac{7}{2}^-)$					$(\frac{7}{2}^-)$
	4.413 [b]			*				
38	4.430					*		
	4.441 [c]							
39	4.464	1	$(\frac{3}{2}^-)$	6	$(\frac{11}{2}^-, \frac{13}{2}^-)$	((0, 1))	$(\frac{1}{2}^\pm, \frac{3}{2}^-)$	†

[a]) Ref. [3]). [b]) Ref. [4]). [c]) Ref. [37]).

* Level observed.

† J-assignment based on shell-model arguments (see text).

†† Closely spaced doublet.

Most probable J^π assignments are listed in the last column.

A comparison of the (d, p) results for states above 3.937 MeV with the previous work is shown in table 5. The energies of some of the levels observed to have similar (d, p) angular distributions of $l = (2, 3)$ appear to correspond to levels reported in the (p, d) study [3]). However, the l-assignments in the two studies are often in disagreement. Possible explanations for these apparent discrepancies are that (i) different states are being excited by the two reactions, or (ii) the l-assignments in one or the other of the studies are in error. With regard to the latter explanation it should be emphasized that unbound states are involved, and the angular distributions are difficult to characterize. However, the different shapes observed in the angular distributions at higher excitation, and the agreement with the (t, p) results for the cases where comparison is possible, suggests that the l-assignments based on the (d, p) reaction are still reasonable. Hence, at least some of the disagreements in the (d, p) and (p, d) studies may indicate that different levels are excited in the two reaction.

In making J^{π} assignments above the neutron binding energy it is not possible to use simple shell-model and weak-coupling arguments which are so helpful at lower energies since both positive-parity and negative-parity 2p-1h states, as well as some 3p-2h states, are expected. The uniformly higher cross sections for the unbound levels compared to the levels at lower excitation probably indicate the onset of the single-particle strength from the next major shell corresponding to $N > 184$. Since this shell is predominantly of negative parity, one expects the single-particle strength to be severely fragmented by the large number of negative-parity 2p-1h states in which the single-particle states are embedded. The high level density observed as well as the large cross sections support this interpretation. Thus in those cases where there is no additional information from other studies, the levels above 3.937 MeV are interpreted as populated via fragments of the single-particle states from the $N > 184$ shell.

Spectroscopic factors. Spectroscopic factors were extracted by fitting the DWBA calculations to the angular distributions measured for the 2p-1h states and using the most probable spin assignments given in tables 4, 5. The results are shown in table 6 where two entries are listed for those cases in which stripping into orbits both above and below the Fermi surface is considered possible. Because of the uncertainties in the form factors discussed previously, the values quoted should be considered uncertain by at least a factor of two. In this regard, certain previous studies are of interest wherein spectroscopic factors extracted using realistic form factors have been compared with those obtained with form factors calculated with the separation-energy prescription [28]). When stripping to a state whose separation energy is smaller than that for the single-particle orbit, as in the case of stripping into the 2p-1h states via an orbit below the Fermi level, the spectroscopic factors obtained using the separation energy prescription are less than the values obtained using the realistic form factor by about a factor of two. The opposite situation is obtained for the case of stripping into a state whose separation energy is greater than that of the single-particle orbit. This would indicate that the spectroscopic factors for stripping via

TABLE 6

Spectroscopic factors from analysis of weak transfers using most probable J^π (see tables 4 and 5) listed for each state together with the assumed configuration

Level no.	E_x	l_n	J^π	$N = 82$–126		$N = 126$–184		$N > 184$		$\left(\frac{d\sigma}{d\Omega}\right)_{max}$ (μb/sr)
				config.	S	config.	S	config.	S	
	0	4	$\frac{9}{2}^+$			$2g_{\frac{9}{2}}$	0.83			4500
	0.779	6	$\frac{11}{2}^+$			$1i_{\frac{11}{2}}$	0.86			500
	1.424	7	$\frac{15}{2}^-$			$1j_{\frac{15}{2}}$	0.58			470
	1.565	2	$\frac{5}{2}^+$			$3d_{\frac{5}{2}}$	0.98			8500
	2.033	0	$\frac{1}{2}^+$			$4s_{\frac{1}{2}}$	0.98			2750
1	2.152	1	$\frac{1}{2}^-$	$3p_{\frac{1}{2}}^{-1}$	0.0067			$4p_{\frac{1}{2}}$	0.0036	18
2	2.319	1	$(\frac{3}{2}^-)$	$3p_{\frac{3}{2}}^{-1}$	0.0074			$4p_{\frac{3}{2}}$	0.0045	45
3	2.424									10
4	2.461	(3)*	$(\frac{5}{2}^-)$	$2f_{\frac{5}{2}}^{-1}$	0.0012			$3f_{\frac{5}{2}}$	0.0013	7
	2.493	4	$\frac{7}{2}^+$			$2g_{\frac{7}{2}}$	1.05			5000
	2.537	2	$\frac{3}{2}^+$			$3d_{\frac{3}{2}}$	1.09			6000
5	2.592	5	$(\frac{11}{2}^-)$					$2h_{\frac{11}{2}}$	0.0185	150
6	2.738	3	$\frac{5}{2}^-$	$2f_{\frac{5}{2}}^{-1}$	0.0027			$3f_{\frac{5}{2}}$	0.0005	18
7	2.866	(3)*	$\frac{5}{2}^-$	$2f_{\frac{5}{2}}^{-1}$	0.0010			$3f_{\frac{5}{2}}$	0.0002	8
8	3.026	5	$(\frac{9}{2}^-)$	$1h_{\frac{9}{2}}^{-1}$	0.0090					20
9	3.052	7	$(\frac{15}{2}^-)$			$1j_{\frac{15}{2}}$	0.070			65
10	3.075	1	$(\frac{3}{2}^-)$	$3p_{\frac{3}{2}}^{-1}$	0.0021			$4p_{\frac{3}{2}}$	0.0012	15
11	3.203	(3)	$(\frac{7}{2}^-)$	$2f_{\frac{7}{2}}^{-1}$	0.0012			$3f_{\frac{7}{2}}$	0.0007	13
12	3.309	5	$(\frac{11}{2}^-)$					$2h_{\frac{11}{2}}$	0.0050	65
13	3.365	5	$(\frac{11}{2}^-)$					$2h_{\frac{11}{2}}$	0.0087	120
14	3.389									10
15	3.414									10
16	3.430									13
17	3.490	3	$(\frac{7}{2}^-)$	$2f_{\frac{7}{2}}^{-1}$	0.0017			$3f_{\frac{7}{2}}$	0.0010	13
18	3.556	7	$(\frac{15}{2}^-)$			$1j_{\frac{15}{2}}$	0.032			38
19	3.615									25
20	3.656	3	$(\frac{5}{2}^-)$	$2f_{\frac{5}{2}}^{-1}$	0.0070			$3f_{\frac{5}{2}}$	0.0044	65
21	3.681	(1)	$(\frac{1}{2}^-, \frac{3}{2}^-)$	$3p_{\frac{1}{2}}^{-1}$	0.0048			$4p_{\frac{1}{2}}$	0.0029	10
22	3.716	7	$(\frac{15}{2}^-)$			$1j_{\frac{15}{2}}$	0.032			40
23	3.904	(3)	$(\frac{7}{2}^-)$					$3f_{\frac{7}{2}}$	0.0113	210
24	3.947	(2, 3)						$(3f_{\frac{7}{2}}$	0.0161) †	320
25	3.985	(2, 3)						$(3f_{\frac{7}{2}}$	0.0178) †	360
26	4.008	(2, 3)						$(3f_{\frac{7}{2}}$	0.0070) †	125
27	4.022	(3)	$(\frac{7}{2}^-)$					$3f_{\frac{7}{2}}$	0.0038	70
28	4.075	(2, 3)						$(3f_{\frac{7}{2}}$	0.0030) †	55
29	4.096	(2)	$(\frac{5}{2}^+)$			$3d_{\frac{5}{2}}$	0.012	$(3f_{\frac{7}{2}}$	0.0070) †	130
30	4.112	(2, 3)						$(3f_{\frac{7}{2}}$	0.0125) †	230
31	4.137	(2, 3)						$(3f_{\frac{7}{2}}$	0.0078) †	140
32	4.166	(5)*	$(\frac{11}{2}^-)$					$2h_{\frac{11}{2}}$	0.0023	35
35	4.295	(0, 1)	$((\frac{3}{2}^-))$					$(4p_{\frac{3}{2}}$	0.0931) †	350
39	4.464	(0, 1)	$((\frac{1}{2}^+))$			$(4s_{\frac{1}{2}}$	0.109) †			250

* Fit based on spin assignment of level made in previous studies.

† See discussion in text.

Observed peak cross sections are listed in the last column.

correlations in the ^{208}Pb ground state (i.e. column N = 82–126 in table 6) are underestimated by perhaps a factor of two or more. In those cases where a state is populated through admixtures of single-particle strength from the $N > 184$ shell, the spectroscopic factors are overestimated by perhaps a factor of two. Hence while the spectroscopic factors presented here possess large uncertainties, they do serve the useful purposes of providing limits on the true spectroscopic factors and of providing the trend of the relative values of different transition strengths.

5. Discussion

Studies in the Pb region support the conclusions that 2p-1h states of two distinct characters are found at low excitation in ^{209}Pb; states based on a neutron coupled to the particle-hole core excited states of ^{208}Pb [i.e. (^{208}Pb(J^π)$\otimes nlj$)], and states based on the coupling of a neutron hole to the two-particle multipole pairing states of ^{210}Pb [i.e. (^{210}Pb(J^π)$\otimes nlj^{-1}$)]. Experimental information concerning a number of 2p-1h states of the latter type has been obtained from studies [2–5]) of the ^{210}Pb(p, d)^{209}Pb and ^{207}Pb(t, p)^{209}Pb reactions. However, recalling that inelastic scattering from ^{209}Pb cannot be performed, very little information has been obtained, except indirectly [2–4, 6, 10]) about ^{209}Pb states based on the core-excited states of ^{208}Pb.

The 2p-1h states of the types described above have been used as basis states in the calculations of Hamamoto [6]), and of Bes and Broglia [7]) to predict the level structure of ^{209}Pb. In the Hamamoto calculation only 2p-1h states based on the weak coupling of a neutron to the ^{208}Pb core excitations have been considered, and hence a comparison with the observed levels is somewhat limited. However, the provision for mixing single-particle orbitals from several major shells into the 2p-1h states of ^{209}Pb has been included. In the Bes and Broglia treatment both sets of basis states are included, and thus a more realistic comparison of the theory to the experimental results is possible. However, in this case the single-particle states are limited to the shell $126 \leqq N \leqq 184$ and the hole states to the shell $82 \leqq N \leqq 126$. Both of these model calculations predict that some 2p-1h states should be populated in the ^{208}Pb(d, p)^{209}Pb reaction via admixtures of single-particle strength.

In addition to the single-particle admixtures, the calculations predict the population of certain 2p-1h states via 2p-2h configurations present in the ^{208}Pb ground state. Other calculations such as the particle-hole RPA calculations of Gillet *et al.* [9]) and the two-particle pairing RPA calculations of Vary and Ginocchio [8]) have predicted the necessity of correlations in the ^{208}Pb ground state in order to reproduce the low excitation energies of the collective levels in ^{208}Pb and the enhancement of their electromagnetic and two-particle transfer strengths. These calculations [6–9]) predict that many 2p-2h, 4p-4h, etc. configurations are mixed into the ground state and that no individual configuration has an especially large amplitude. This means that while the coherent effects of correlations, as sampled by inelastic scattering and two-nucleon transfers, may be large, the predicted occupation fractions are

small ($\approx$ 1–5 %) and a direct measurement of the individual 2p-2h configurations, as sampled by the (d, p) reaction for example, will yield small effects. In particular, the calculations of Vary and Ginocchio [8]) as well as those of Hamamoto [6]) and Bes and Broglia [7]), predict that only some of the 2p-1h states will be populated by direct transfer in the (d, p) reaction as a result of 2p–2h correlations, and then only weakly.

In the following sections we compare the experimental results with the model calculations which predict the population of 2p-1h states via a direct one-step transfer mechanism. First the admixture of single-particle strength from the two major shells above the Fermi level at $N = 126$ into the 2p–1h states will be discussed as a mechanism for excitation; then the role of 2p-2h correlations in the ^{208}Pb ground state will be considered, followed by a brief discussion of the possibility of two-step processes contributing to the excitation of 2p-1h states.

5.1. ADMIXTURES OF SINGLE-PARTICLE STATES FROM THE SHELL $126 < N \leqq 184$

The results of the DWBA analysis of the strong transition to the seven single-particle states in the shell $126 < N \leqq 184$ indicate that all of their spectroscopic factors are consistent with unity (within the uncertainties of DWBA), except for the $\frac{15}{2}^-$ state at 1.424 MeV with a spectroscopic factor of $S \approx 0.6$–0.7. The fragmentation of $j_{\frac{15}{2}}$ strength has been interpreted [32]) as arising from the interaction with the $\frac{15}{2}^-$ member of the $(^{208}\mathrm{Pb}(3^-)\otimes g_{\frac{9}{2}})$ multiplet, and this interpretation is supported by the observation that the γ-decay strength of the 1.424 MeV level is strongly enhanced over the single-particle value for a $j_{\frac{15}{2}}$ state [33]). The location of the missing $j_{\frac{15}{2}}$ strength which is presumably mixed into states at higher excitation, is a matter of considerable interest. The level at 3.309 MeV was previously suggested [10]) as a candidate for $j_{\frac{15}{2}}$ strength. In the present experiment this level was observed to be populated by an $l = 5$ transfer. That fact together with the results of the (t, p) study [4]) implies a spin-parity of $\frac{11}{2}^-$ for the 3.309 MeV level and denies the suggestion of ref. [10]). However, in addition to the level at 1.424 MeV ($S = 0.77$), three $l = 7$ assignments are made for (d, p) transitions in the present work. The corresponding states are at 3.052 MeV ($S = 0.09$), 3.556 MeV ($S = 0.04$), and 3.716 MeV ($S = 0.04$), and they are the best candidates for the missing $j_{\frac{15}{2}}$ strength. The sum of the $j_{\frac{15}{2}}$ spectroscopic strength contained in these four levels is 0.94 based on analysis with the deuteron breakup potential, and within the uncertainties of the analysis, this value exhausts the sum rule. Assuming that all the $j_{\frac{15}{2}}$ strength has been located, the $1j_{\frac{15}{2}}$ centroid lies at $E_x = 1.776$ MeV.

The distributions of $j_{\frac{15}{2}}$ strength predicted by the calculations of Hamamoto [6]), and of Bes and Broglia [7]) are compared with the observed fragmentation in table 7. In addition to the four levels assigned $\frac{15}{2}^-$ in the present study, there are two other possible $\frac{15}{2}^-$ levels in this excitation region based on the results of the (t, p) study [4]). These are the levels at 3.100 MeV, not observed in (d, p), and the level at 3.430 MeV, weakly observed. The structure of the 3.430 MeV level has previously been inter-

TABLE 7

Comparison of experimental and theoretical excitation energies and spectroscopic factors for states containing $j_{\frac{15}{2}}$ single-particle strength

Experiment		Bes and Broglia [a]			Hamamoto [b]		
E_x (MeV)	S	E_x (MeV)	S	primary configuration	E_x (MeV)	S	primary configuration
1.424	0.770	1.41	0.650	$(0^+\otimes j_{\frac{15}{2}})$	1.41	0.645	$(0^+\otimes j_{\frac{15}{2}})$
3.052	0.090	3.22	0.166	$(3^-\otimes g_{\frac{9}{2}})$, $(3^-\otimes i_{\frac{13}{2}})$	3.21	0.255	$(3^-\otimes g_{\frac{9}{2}})$
(3.430) [c]	(0.010)	3.32	0.001	$(^{210}\text{Pb}(8^+)\otimes p_{\frac{1}{2}}^{-1})$	3.18	0.041	$(5_1^-\otimes g_{\frac{9}{2}})$
3.556	0.042	3.47	0.304	$(3^-\otimes g_{\frac{9}{2}})$, $(3^-\otimes i_{\frac{13}{2}})$	3.47	0	$(3^-\otimes i_{\frac{13}{2}})$
3.716	0.042	3.85	0.002				

[a]) Ref. [7]).
[b]) Ref. [6]).
[c]) Not identified as $l = 7$ transition in this study. See text.

preted [4]) as a predominantly $(^{210}\text{Pb}(8^+)\otimes p_{\frac{1}{2}}^{-1})_{J^\pi=\frac{15}{2}^-}$ configuration. Even though the (d, p) angular distribution associated with this level is more characteristic of a small-l transfer than an $l = 7$, this level has been included in table 7 to make as fair a comparison as possible of theory [7]) to experiment. If the level is fit by $l = 7$, a spectroscopic factor of $S(j_{\frac{15}{2}}) = 0.010$ is obtained; however, the fit is very poor. We conclude from table 7 that although each of the model calculations predicts some fragmentation of $j_{\frac{15}{2}}$ strength, neither of them reproduces accurately the splitting of strength that is observed.

No unambiguous evidence for fragments of positive-parity strength corresponding to the other single-particle states in the shell $126 < N \leqq 184$ was found. Model calculations by Hamamoto and by Bes and Broglia predict that fragments of positive-parity single-particle strength should be found in the excitation region of 4.0 to 5.0 MeV. However, the high level densities and the uncertainties in the l-assignments make it difficult to draw any definite conclusions. Two possible candidates for states with single-particle strength are the levels at 4.096 MeV $(\frac{5}{2}^+)$ and 4.464 MeV $(\frac{1}{2}^+)$. The excitation energies and spectroscopic factors extracted are in reasonable agreement with the predictions of both Hamamoto, and Bes and Broglia.

5.2. ADMIXTURES OF SINGLE-PARTICLE STATES FROM THE SHELL $N > 184$

The experimental results provide evidence that single-particle strength from the second neutron shell above the Fermi surface (predominantly of negative parity) may be found in some of the 2p-1h states in the excitation region below 3.90 MeV. The most unambiguous evidence comes from the observation of the four $l = 5$ transfers to levels at 2.592, 3.026, 3.309, and 3.365 MeV. For the two levels at 3.026

and 3.309 MeV there is additional spin information from the (t, p) reaction permitting J^π assignments of $\frac{9}{2}^-$ and $\frac{11}{2}^-$, respectively. The other two levels at 2.592 and 3.365 MeV were given tentative $\frac{11}{2}^-$ spin assignments based on the argument that unreasonably large spectroscopic factors are obtained for $2h_{\frac{9}{2}}$ strength [$S(h_{\frac{9}{2}}) = 0.09$ and 0.05] if a $\frac{9}{2}^-$ assignment is assumed, even allowing for large uncertainties in the extracted values. This interpretation is supported by the theoretical calculations of Hamamoto. In Hamamoto's calculation the possibility of admixtures of single-particle states from this shell is included; and, in particular, the calculation predicts the admixture of $2h_{\frac{11}{2}}$ strength in the $\frac{11}{2}^-$ member of the $(^{208}\text{Pb}(3^-)\otimes g_{\frac{9}{2}})$ multiplet. The predicted excitation energy at 2.61 MeV, and mixing probability of 0.027, are in good agreement with the level observed at 2.592 MeV with a spectroscopic factor of $S(h_{\frac{11}{2}}) = 0.0185$. In addition, the two smaller fragments of $h_{\frac{11}{2}}$ strength predicted to be mixed into the $\frac{11}{2}^-$ members of the $(^{208}\text{Pb}(3^-)\otimes i_{\frac{13}{2}})$ and $(^{208}\text{Pb}(5_1^-)\otimes g_{\frac{9}{2}})$ particle-core coupled states at excitation of 3.4 and 3.2 MeV, respectively, can be reasonably associated with the levels at 3.365 and 3.309 MeV. The calculations of Bes and Broglia, and of Vary and Ginocchio do not include the possibility of single-particle admixtures from the shell $N > 184$ and hence are not able to account for the large strengths observed for the $l = 5$ transfers.

With evidence for $2h_{\frac{11}{2}}$ strength mixed into several 2p-1h states, one might expect strength from other negative-parity states from this shell mixed into a number of 2p-1h states at low excitation. Unfortunately, the experimental results cannot answer the question directly for two reasons. First, in the calculation of Hamamoto, no radial quantum numbers are specified, and the mixing probability of $p_{\frac{1}{2}}$ strength, for example, contains contributions from all $p_{\frac{1}{2}}$ orbitals including filled and unfilled ones, e.g. $3p_{\frac{1}{2}}$ and $4p_{\frac{1}{2}}$. Hence it is not possible to distinguish between spectroscopic strength arising from correlations in the ground state as opposed to admixtures of single-particle strength from the $N > 184$ shell. (The $h_{\frac{11}{2}}$ strength discussed previously is an exception since the $1h_{\frac{11}{2}}$ orbital is sufficiently far below the Fermi level to ignore its contribution.) Second, with the exception of several levels below 3 MeV and the three levels above 3 MeV that were assigned $j_{\frac{15}{2}}$, it is difficult to specify experimentally the precise structure of many of the 2p-1h excitations and consequently difficult to draw a correspondence between experimental and theoretical states. Therefore admixtures of single-particle strength beyond what has been mentioned thus far are possible and cannot be ruled out without more detailed studies.

5.3. CORRELATIONS IN THE GROUND STATE OF ^{208}Pb

In the excitation region below 3.0 MeV in ^{209}Pb seven 2p-1h states were observed in the study of the (t, p) and (p, d) reactions. The results from these studies are sufficient to construct wave functions for these states, using the spectroscopic factors and cross sections measured in the two reactions and making certain simplifying assumptions about the available configurations. These empirical wave functions allow one to test directly predicted wave functions for ^{209}Pb as well as predictions

TABLE 8

Comparison of spectroscopic factors predicted by RPA [8]) with those measured for 2p-1h states below 3.00 MeV

J^π	E_x (MeV)	(p, d) [a])		(t, p) [b])		Wave functions			Spectroscopic factors		
		l	S_{exp}	L	$\frac{\sigma(209)}{\sigma(210)}$	^{210}Pb$(0^+)\otimes l_j^{-1}$	^{210}Pb$(2^+)\otimes p_{\frac{1}{2}}^{-1}$	^{208}Pb$(3^-)\otimes g_{\frac{9}{2}}$	l	exp	theory [c])
$\frac{1}{2}^-$	2.152	1	2.00	0	1.02	$\sqrt{1.0}(0^+\otimes p_{\frac{1}{2}}^{-1})$			1	0.0067	0.0043
$\frac{3}{2}^-$	2.319	1	0.56			$\sqrt{0.14}(0^+\otimes p_{\frac{3}{2}}^{-1})$		$\sqrt{0.85}(3^-\otimes g_{\frac{9}{2}})$	1	0.0074	0.0076±0.0030
$\frac{3}{2}^-$	2.906	1	0.26	2	0.38	$\sqrt{0.07}(0^+\otimes p_{\frac{3}{2}}^{-1})$	$\sqrt{0.95}(2^+\otimes p_{\frac{1}{2}}^{-1})$				0.0007±0.0006
$\frac{3}{2}^-$	3.075	1	3.16			$\sqrt{0.78}(0^+\otimes p_{\frac{3}{2}}^{-1})$			(1)	0.0021	0.0017
$\frac{5}{2}^-$	2.461	3	0.81			$\sqrt{0.14}(0^+\otimes f_{\frac{5}{2}}^{-1})$		$\sqrt{0.85}(3^-\otimes g_{\frac{9}{2}})$	(3)	0.0012	0.0015±0.0015
$\frac{5}{2}^-$	2.730	3	4.06	2	0.25	$\sqrt{0.69}(0^+\otimes f_{\frac{5}{2}}^{-1})$	$\sqrt{0.42}(2^+\otimes p_{\frac{1}{2}}^{-1})$		3	0.0027	0.0031±0.0017
$\frac{5}{2}^-$	2.866	3	1.02	2	0.38	$\sqrt{0.18}(0^+\otimes f_{\frac{5}{2}}^{-1})$	$\sqrt{0.63}(2^+\otimes p_{\frac{1}{2}}^{-1})$		(3)	0.0010	0.0011±0.0011

The empirical wave functions derived from (p, d) and (t, p) studies and used in the theoretical calculation are shown.

[a]) Ref. [3]).

[b]) Ref. [4]).

[c]) Ref. [8]).

of the correlations in the ^{208}Pb ground state by use of the spectroscopic factors for populating these states in the (d, p) reactions.

In table 8 are shown the empirical wave functions attributed by Vary and Ginocchio [ref. [8])] to the seven 2p-1h states below 3.0 MeV which have been used to calculate the spectroscopic factors [8]) based on 2p-2h correlations in the ^{208}Pb ground state. The results of the (t, p) and (p, d) studies are summarized in the table. More levels are observed in this region than can be constructed with 2p-1h states of $(^{210}\mathrm{Pb}(J^{\pi})\otimes nlj^{-1})$ character, and the only other states at this excitation which might be expected to mix with these states are the $\frac{3}{2}^-$ and $\frac{5}{2}^-$ members of the $(^{208}\mathrm{Pb}(3^-)\otimes g_{\frac{9}{2}})$ multiplet. Thus in table 8, the first two contributions to the wave functions are determined from the (t, p) and (p, d) experiments and the third contribution is determined by requiring that the $[^{208}\mathrm{Pb}(3^-)\otimes g_{\frac{9}{2}}]$ configuration exhaust the remaining part of each wave function. Given a ground-state wave function, it is possible to calculate spectroscopic factors for (d, p) transitions to these states. The theoretical spectroscopic factors in the table are based on the 1p-1h RPA calculations of Gillet *et al.* [9]) and the 2p pairing RPA calculations of Vary and Ginocchio [8]). The large error bars on the theoretical predictions result from the unknown phases of the amplitudes of the different empirical configurations. The agreement with the spectroscopic factors obtained in this study is excellent. It must be remembered, however, that the experimental spectroscopic factors have large uncertainties and, for stripping into the core, may be larger by perhaps a factor of two. In view of these uncertainties, agreement within a factor of two to four would be considered good, and the detailed agreement observed in table 8 must be considered fortuitous. The crucial point to emphasize is that both the trend and the approximate magnitudes are reproduced by the calculations and thus consistent with the existence of ground-state correlations.

In table 9 the predictions of the Bes and Broglia calculation are compared with the results of the (p, d), (t, p) and (d, p) reactions. For the (d, p) reaction, the predictions can be considered to be in reasonable agreement with the experimental spectroscopic factors, except for the $\frac{3}{2}^-$ and $\frac{5}{2}^-$ states at 2.319 and 2.461 MeV with dominant configuration $(^{208}\mathrm{Pb}(3^-)\otimes g_{\frac{9}{2}})$ which are predicted to be about an order of magnitude larger than observed. Again, the experimental results are consistent with the existence of ground-state correlations.

In table 10 are listed the predicted excitation energies of the $(^{208}\mathrm{Pb}(3^-)\otimes g_{\frac{9}{2}})$ septuplet with the single-particle mixing probabilities predicted by Hamamoto and the spectroscopic factors predicted by Bes and Broglia. The comparison with experiment is limited to four states since no levels corresponding to the $\frac{7}{2}^-$, $\frac{9}{2}^-$, or $\frac{13}{2}^-$ members of the multiplet were observed. The level observed at 2.424 MeV in the present study could possibly be either the $\frac{9}{2}^-$ or $\frac{13}{2}^-$ member; however, it was too weakly excited to permit an *l*-assignment in this study. The $\frac{7}{2}^-$ member of the multiplet, tentatively identified in the ^{210}Pb(p, d)^{209}Pb study to be at 2.563 MeV, was not seen in this (d, p) study because of the strongly populated $3d_{\frac{5}{2}}$ state located nearby. As can be noted from table 10, the excitation-energy predictions of Hamamoto, and of Bes and Broglia

TABLE 9

Comparison of spectroscopic factors and cross-section strengths for the (p, d), (d, p) and (t, p) reactions predicted by Bes and Broglia [7]) with those measured

	Excitation energy (MeV)		^{210}Pb(p, d) spectroscopic factors		^{207}Pb(t, p) [b]) $\sigma_{exp}/\sigma_{theory}$ norm	^{208}Pb(d, p) spectroscopic factors	
	exp	theory [d])	exp [a])	theory [d])		exp [c])	theory [d])
$\frac{1}{2}^-$	2.152	2.223	2.15	1.83	1.00	0.0067	0.0090
$\frac{3}{2}^-$	2.319	2.36	0.50	1.21		0.0074	0.0630
$\frac{3}{2}^-$	2.906	2.979	0.20	0.20	0.63		0
$\frac{3}{2}^-$	3.075	3.19	2.60	2.60		0.0021	0
$\frac{5}{2}^-$	2.461	2.37	0.61	0.51		0.0012	0.0100
$\frac{5}{2}^-$	2.738	2.786	4.75	5.21	6.10	0.0027	0.0060
$\frac{5}{2}^-$	2.866	2.983	1.02	0.08	0.52	0.0010	0.0040

[a]) Ref. [3]).
[b]) Ref. [4]).
[c]) Present study.
[d]) Ref. [7]).

TABLE 10

Comparison of the predicted excitation energies of the (^{208}Pb(3^-)$\otimes g_{\frac{9}{2}}$) multiplet and expected spectroscopic factors with those states identified in experiment

Spin J^π	Excitation energies			Spectroscopic factors		
	exp	Hamamoto [a])	Bes and Broglia [b])	exp	Hamamoto [a])	Bes and Broglia [b])
$\frac{3}{2}^-$	2.319	2.37	2.36	0.0074	0.037	0.063
$\frac{5}{2}^-$	2.461	2.35	2.37	0.0012	0.004	0.010
$\frac{7}{2}^-$	(2.563) [c])	2.66	2.61	[d])	0.015	0.014
$\frac{9}{2}^-$		2.46	2.47		0.002	0.001
$\frac{11}{2}^-$	2.592	2.61	2.68	0.0185	0.027	0.001
$\frac{13}{2}^-$		2.49	2.51		0.001	0.000
$\frac{15}{2}^-$	3.052	3.21	3.22	0.0520	0.255	0.166

[a]) Ref. [6]).
[b]) Ref. [7]).
[c]) Observed in the (p, d) reaction [3]).
[d]) Obscured by nearby intense group in the (d, p) reaction.

are essentially identical and are in good agreement with the members which have been observed. The Hamamoto mixing probabilities listed in table 10 include single-particle components corresponding to stripping into orbits both in the core and continuum, while Bes and Broglia's spectroscopic factor includes only the effect of correlations in the ^{208}Pb ground state and hence stripping into the core. The difference in predictions for the $\frac{11}{2}^-$ member discussed previously is significant. This is the only one of the four measured spectroscopic factors which agrees well with either calculation (Hamamoto), and it supports the $h_{\frac{11}{2}}$ single-particle admixture. All of the other

TABLE 11

Comparison of experimental and theoretical spectroscopic factors [7]) and the energies of levels excited in the ^{208}Pb(d, p)^{209}Pb reaction

Level no.	Excitation energies		Spin J^π	^{208}Pb(d, p)^{209}Pb		
	exp.	theory [a])		l	S_{exp}	S_{th} [a])
1	2.152	2.22	$\frac{1}{2}^-$	1	0.0067	0.0090
2	2.319	2.40	$(\frac{3}{2}^-)$	1	0.0074	0.0630
3	2.424	(2.49)	$((\frac{9}{2}^-))$			0.0010
4	2.461	2.90	$(\frac{9}{2}^-)$	(3)	0.0012	0.0100
5	2.592	2.68	$(\frac{11}{2}^-)$	(5)	0.0185	
6	2.738	2.79	$\frac{5}{2}^-$	3	0.0027	0.0060
7	2.866	2.98	$\frac{5}{2}^-$	(3)	0.0010	0.0040
8	3.026	3.21	$\frac{9}{2}^-$	(5)	0.0090	0.0010
9	3.052	3.22	$(\frac{15}{2}^-)$	7	0.0520	0.1700
10	3.075 [b])	3.21	$(\frac{3}{2}^-, \frac{13}{2}^-)$	1	0.0021	0.0000
11	3.203	3.22	$\frac{7}{2}^-$	(3)	0.0012	0.0003
12	3.309	3.28	$\frac{11}{2}^-$	(5)	0.0050	
13	3.365	3.32	$\frac{11}{2}^-$	(5)	0.0087	
14	3.389					
15	3.414					
16	3.430	3.32	$(\frac{15}{2}^-)$	(7)	0.0060	0.0010
17	3.490		$(\frac{7}{2}^-)$	(3)	0.0017	0.0020
18	3.556	3.47	$(\frac{15}{2}^-)$	7	0.0280	0.3040
19	3.615					
20	3.656 [b])	3.41	$\frac{5}{2}^-, \frac{13}{2}^+$	3	0.0070	0.0240
21	3.681	3.83	$(\frac{1}{2}^-)$	1	0.0048	0.0160
22	3.716	3.85	$(\frac{15}{2}^-)$	7	0.0270	0.0020

[a]) Ref. [7]).

[b]) Experimental results indicate that two closely spaced levels of the spins and parities listed are found at these excitations.

spectroscopic factors are predicted to be much larger than observed, with the calculation of Hamamoto perhaps somewhat closer overall than that of Bes and Broglia.

All of the spectroscopic factors predicted by the Bes and Broglia calculation for levels up to 4.0 MeV are compared in table 11 to those observed in this study. For purposes of comparison, theoretical and experimental levels of appropriate spin are simply matched according to their energy if no additional information is available. It is difficult to draw conclusions from the comparisons at excitation energies above 3.0 MeV, except to stress that of the rather large number of 2p-1h states expected in the excitation region, relatively few are predicted to have significant spectroscopic factors. Indeed, this is what is observed. Furthermore, within approximately 100 keV of most levels predicted to be seen in the (d, p) reaction, there is an observed level. However, upon closer inspection some exceptions to this agreement can be found. For example, the states at 3.026 and 3.202 MeV, identified in the (t, p) study to be of

predominantly (^{210}Pb(4^+)$\otimes p_{\frac{1}{2}}^{-1}$) configuration, are observed in the (d, p) reaction, while theoretically they are predicted to have zero spectroscopic factors. Other exceptions to the agreement are the three relatively strong $\frac{11}{2}^-$ states which are not predicted to be populated. This is consistent with the interpretation that these states are populated via $N > 184$ shell single-particle admixtures not included in the Bes and Broglia calculation. In view of the uncertain identification of individual levels, and the uncertainties in the experimental spectroscopic factors, it seems reasonable to conclude only that there is qualitative agreement concerning the number of 2p-1h states excited, and order-of-magnitude agreement concerning the spectroscopic factors.

5.4. COMMENTS ON REACTION MECHANISM

Thus far we have made only brief mention of the possibility of a reaction mechanism more complex than a simple one-step stripping process. In this study, the 2p-1h states were assumed to be populated by a direct one-step transfer and the data analyzed accordingly. This assumption is not without basis since structure calculations indicate that 2p-1h states in ^{209}Pb should be populated by direct transfer and, indeed, the experimental angular distributions as well as the order of magnitude of the cross sections are consistent with such an interpretation. While there is nothing in the experimental data or analysis which would strongly indicate contributions from higher-order processes, this does not prove that two-step processes are not important. Theoretical calculations of two-step reactions indicate that in many cases their contributions to the cross sections are not negligible, especially in the cases of weak transitions leading to states with favorable parentage.

The 2p-1h states studied here have two distinctly different parentages which might favor two different kinds of two-step processes. The 2p-1h states based primarily on the core-excited states of ^{208}Pb are expected to be most strongly populated by two-step processes involving a strong inelastic channel. Such mechanisms have been shown to be important in reactions on deformed targets [34, 35]). The 2p-1h states based primarily on the two-particle multipole pairing states of ^{210}Pb would appear to favor population by a sequential transfer (e.g. d → t → p). This type of mechanism has been able to reproduce rather successfully the anomalous angular distributions observed for some weak transitions in the ^{210}Pb(p, d)^{209}Pb reaction [36]).

In the present study, 2p-1h states of both parentages are excited along with other states for which the primary 2p-1h configurations are not known. Calculations of two-step processes have not been performed for the ^{208}Pb(d, p)^{209}Pb reaction thus far, but it would be very interesting to know the importance of such contributions, particularly with respect to this wide range of 2p-1h states observed experimentally. It should be stressed that the empirical wave functions presented in table 8 for the low-lying 2p-1h states provide an excellent opportunity to test the reaction mechanism, and it is hoped that data obtained here will stimulate such calculations.

6. Summary of conclusions

This work shows that a substantial number of 2p-1h states are excited in ^{209}Pb by the (d, p) reaction with cross sections a factor of 10 to 100 less than the strong single-particle states. Many of the same 2p-1h states are observed with relatively large cross sections in the (t, p) and (p, d) reactions leading to ^{209}Pb, a fact which confirms their 2p-1h structure. In each case where spin and parity information is available from previous experiments, the (d, p) angular distribution proves to be consistent with the DWBA calculation based on the *l*-value that would be assigned for a direct neutron-stripping process. While this does not rule out excitation by a more complicated reaction mechanism involving perhaps multistep processes, it does suggest that one should initially attempt to understand the data in terms of a one-step transfer process until the more complicated calculations can be carried out. For a number of levels, it was possible to make actual spin and parity assignments based on the *l*-value extracted from the (d, p) reaction together with the angular momentum transfer that was measured in one of the "2p-1h reactions".

There are two possible ways to interpret the spectroscopic strength leading to 2p-1h states. Such strength may be a measure of possible single-particle admixtures, or else it may arise from 2p-2h correlations in the ^{208}Pb ground state. Both possibilities were examined for each of the levels, and in some cases conclusions could be reached as to the most likely source of the strength. The most important conclusion about the fragmentation of single-particle strength concerns the $j_{\frac{1}{2}}$ orbital for which three fragments are now established in the region 3–4 MeV, in addition to the previously known large one at 1.424 MeV. Another significant single-particle fragment in the region below 4 MeV appears to correspond to about 2 % of the $2h_{\frac{1}{2}}$ orbital which belongs to the $N > 184$ shell. Above 4 MeV there is considerable (d, p) strength fragmented into many levels, signifying the onset of the $N > 184$ major shell.

The best evidence for direct observation of 2p-2h admixtures in the ^{208}Pb ground state is the population of the negative-parity 2p-1h states between 2 and 3 MeV excitation by the (d, p) reaction. As shown in table 8 there are seven states with spins known from the "2p-1h reactions" for which empirical wavefunctions can be constructed, and the RPA calculation of Vary and Ginocchio predicts spectroscopic factors for exciting these states due to 2p-2h admixtures. In each case the experimental angular distribution agrees fairly well with the *l*-value for direct transfer implied by the spin and parity of the states, and the spectroscopic strength agrees with the trend of the calculated values. The fact that the individual spectroscopic factors are all less than 1 % would normally generate considerable skepticism in attempting to interpret them. In the present case, however, the emphasis is not on any individual transition or extracted value, but on the overall consistent picture that emerges when the (d, p) results are compared with the previous "2p-1h experiments" and with the theoretical calculations. Thus we conclude that the (d, p) cross sections to at least some of the 2p-1h states are consistent with 2p-2h admixtures in the ^{208}Pb ground

state amounting to several tenths of a percent for individual configurations and possibly amounting to tens of percent in total.

So far as is known, the present effort represents the first attempt to measure and to analyze systematically the weak 2p-1h excitations observed over a broad energy range in a (d, p) reaction. The analysis presented here represents the simplest approach and the interpretation encompasses many qualitative aspects and uncertainties. Analyses using realistic form factors and including contributions from possible multistep processes would certainly be of great value in providing more definite answers to the questions raised here. However, the qualitative aspects and uncertainties in the analysis and interpretation of these results should not detract from the broader conclusion to be drawn from this study, namely, that the weak transitions in the (d, p) and possibly other direct reactions provide potentially fertile ground for exploring some of the more subtle features of nuclear structure than have heretofore been accessible with the stronger transitions.

We would like to thank W. Callender, C. A. Maguire, L. McVay and W. Metz for help in taking the data. Helpful discussions with R. Ascuitto, J. Ginocchio, and J. Vary are acknowledged. The support and encouragement of Professors Bromley and Parker are deeply appreciated. The members of the Wright Nuclear Structure Laboratory staff are thanked for their help and cooperation, especially the members of the scanning group for their excellent reading of the spectrograph plates.

References

1) D. A. Bromley and J. Weneser, Comm. Nucl. Part. Phys. **11** (1968) 51;
N. Stein, Proc. Int. Conf. on properties of nuclear states, Montreal, ed. M. Harvey (Univ. of Montreal Press, 1969)
2) E. R. Flynn, G. Igo, P. D. Barnes and D. Kovar, Phys. Rev. Lett. **22** (1969) 142
3) G. Igo, E. R. Flynn, D. J. Dropesky and P. D. Barnes, Phys. Rev. **C3** (1971) 349
4) E. R. Flynn, G. Igo, P. D. Barnes, D. Kovar, D. Bes and R. Broglia, Phys. Rev. **C3** (1971) 2371
5) J. H. Bjerregaard, O. Hansen, O. Nathan, L. Vistisen, R. Chapman and S. Hinds, Nucl. Phys. **A113** (1968) 484
6) I. Hamamoto, Nucl. Phys. **A126** (1969) 545; **A141** (1970) 11
7) D. Bes and R. Broglia, Phys. Rev. **C3** (1971) 2389
8) J. Vary and J. Ginocchio, Nucl. Phys. **A166** (1971) 479
9) V. Gillet, A. M. Green and E. A. Sanderson, Nucl. Phys. **88** (1966) 321;
D. Agassi, V. Gillet and A. Lumbrosco, Nucl. Phys. **A130** (1969) 129
10) C. Ellegaard, J. Kantele and P. Vedelsby, Nucl. Phys. **A129** (1969) 113
11) A. F. Jeans, W. Darcey, W. E. Davies and P. K. Smith, Nucl. Phys. **A128** (1969) 224
12) G. J. Igo, P. D. Barnes, E. R. Flynn and D. D. Armstrong, Phys. Rev. **177** (1969) 1831
13) D. G. Kovar, C. K. Bockelman, W. D. Callender, L. J. McVay, C. F. Maguire and W. D. Metz, Wright Nuclear Structure Laboratory Report 49, Yale University (unpublished)
14) J. H. E. Mattauch, W. Thiele and A. H. Wapstra, Nucl. Phys. **67** (1965) 1
15) G. Muehllehner, A. S. Poltorak, W. C. Parkinson and R. H. Bassel, Phys. Rev. **159** (1967) 1039
16) P. D. Kunz, unpublished
17) L. L. Lee, Jr., J. P. Schiffer, B. Zeidman, G. R. Satchler, R. M. Drisko and R. H. Bassel, Phys. Rev. **136** (1964) B971

18) G. R. Satchler, Nucl. Phys. **55** (1964) 1
19) E. H. Auerbach, private communication
20) G. R. Satchler, Nucl. Phys. **A92** (1967) 273
21) F. G. Perey, Nuclear spectroscopy with direct reactions, ANL-6848 (1969) 114
22) G. R. Satchler, Phys. Rev. **C4** (1971) 1485
23) M. Dost and W. R. Hering, Phys. Lett. **26B** (1968) 443
24) C. J. Batty, Phys. Lett. **31B** (1970) 496
25) M. H. Macfarlane, Proc. Int. Conf. on properties of nuclear states, Montreal, ed. M. Harvey (Univ. of Montreal Press, 1969)
26) W. T. Pinkston and G. R. Satchler, Nucl. Phys. **72** (1965) 641
27) W. T. Pinkston, R. I. Philpott and G. R. Satchler, Nucl. Phys. **A125** (1969) 176; J. L. Hutton, Nucl. Phys. **A120** (1968) 657
28) R. J. Philpott, W. T. Pinkston and G. R. Satchler, Nucl. Phys. **A119** (1968) 241
29) D. G. Kovar, Ph.D. Thesis, Yale University (unpublished)
30) R. C. Johnson and P. J. R. Soper, Phys. Rev. **C1** (1970) 976
31) C. A. Whitten, N. Stein, G. E. Holland and D. A. Bromley, Phys. Rev. **188** (1969) 1941
32) B. R. Mottelson, Int. Conf. on nuclear structure, Tokyo (1967) p. 96
33) C. Ellegaard, J. Kantele and P. Vedelsby, Phys. Lett. **25B** (1967) 512
34) R. J. Ascuitto, C. H. King and L. J. McVay, Phys. Rev. Lett. **29** (1972) 1106
35) L. J. McVay, R. J. Ascuitto and C. H. King, Phys. Lett. **43B** (1973) 119
36) M. Igarashi, M. Kawai and K. Yazaki, Phys. Lett. **42B** (1972) 323
37) G. C. Kyker, Jr., E. G. Bilpuch, J. A. Farrell and H. W. Newson, Bull. Am. Phys. Soc. **7** (1962) 289
38) E. G. Bilpuch, K. K. Seth, C. D. Bowman, R. H. Tabony, R. C. Smith and H. W. Newson, Ann. of Phys. **14** (1961) 387
39) R. E. Peterson, R. K. Adair and H. H. Barshall, Phys. Rev. **79** (1950) 935
40) J. L. Fowler and E. C. Campbell, Phys. Rev. **127** (1962) 2192